Stereoselective Propene Insertion Reactions of *rac*-(EBI)Zr(η^2-pyridyl)$^+$ Complexes

Samuel Dagorne, Stephan Rodewald, and Richard F. Jordan*

Department of Chemistry, The University of Iowa, Iowa City, Iowa 52242

Received August 21, 1997[⊗]

Stereoselective propene insertion reactions of chiral zirconocene species of the type *rac*-(EBI)Zr(η^2-pyridyl)$^+$ (EBI = ethylenebis(indenyl)) containing substituted η^2-pyridyl ligands are described. The reaction of *rac*-(EBI)ZrMe$_2$ with B(C$_6$F$_5$)$_3$ followed by addition of 1 equiv of the appropriate pyridine yields [*rac*-(EBI)Zr(η^2-3-R^3-5-R^5-6-R^6-pyrid-2-yl)][MeB(C$_6$F$_5$)$_3$] pyridyl complexes (**5a**−**f**; **a**, R^3 = R^5 = H, R^6 = Me; **b**, R^3 = R^5 = H, R^6 = Ph; **c**, R^3 = R^5 = R^6 = H; **d**, R^3 = Me, R^5 = H, R^6 = Me; **e**, R^3 = H, R^5 = R^6 = Me; **f**, R^3 = R^5 = Me, R^6 = H). At 23 °C, **5a**−**f** react with propene to yield the 1,2-insertion products [*rac*-(EBI)Zr{η^2(*C*,*N*)-CH$_2$CHMe(pyrid-2-yl)}][MeB(C$_6$F$_5$)$_3$], for which two diastereomers (**6**/**6′**) that differ in the configuration of the metallacycle β-carbon are possible. Propene insertion of **5a**−**f** is under kinetic control at 23 °C and is highly stereoselective when the pyridyl ring contains a 6-substituent (R^6 ≠ H; **6a**, de = 80%; **6b**, de > 96%; **6d**, de > 96%; **6e**, de = 80%). For these cases, the major diastereomer is that in which the metallacycle β-Me group points toward the EBI C$_6$ ring (configuration *S*,*S*,*S* (*R*,*R*,*R*), where the entries denote the configurations of the EBI bridgehead carbons and the metallacycle β-carbon, respectively). The diastereoselectivity is low in cases where R^6 = H (**6c′**, de = 20%; **6f**, de = 10%). Propene insertion of **5a**−**f** is reversible at 80 °C, and the kinetic **6**/**6′** mixtures evolve to the thermodynamic mixtures at this temperature. **6d** isomerizes to a mixture of **6d**, **6d′**, and the 2,1-insertion product [*rac*-(EBI)Zr{η^2(*C*,*N*)-CHMeCH$_2$(pyrid-2-yl)}][MeB(C$_6$F$_5$)$_3$] (**6d″**) at 80 °C. Molecular modeling calculations for model *rac*-(EBI)Zr(η^2-pyridyl)(propene)$^+$ species suggest that steric interactions between the pyridyl R^6 substituent and the EBI C$_6$ ring cause a tipping of the pyridyl ligand, which influences the pyridyl/propene steric contacts and the facial selectivity of propene binding. The modeling calculations also suggest that the more stable propene adduct diastereomer leads to the kinetic insertion product.

Introduction

Cationic zirconocene alkyl complexes of general type Cp$_2$Zr(R)(L)$_n^+$ (n = 0, 1; L = labile ligand) react readily with pyridines and other N-heterocycles by coordination and metalation (ortho C−H activation) to yield η^2-pyridyl complexes **1**, which may be trapped as the pyridine complexes **2**/**2′** (Scheme 1).[1,2] The η^2-pyridyl complexes **1** are quite reactive and insert α-olefins and other unsaturated substrates to yield ring-expanded products. The α-olefin insertions proceed regiospecifically to yield 1,2-insertion products **3**, in which a stereogenic center is present at the β-position (versus Zr) of the metallacycle.

Scheme 1

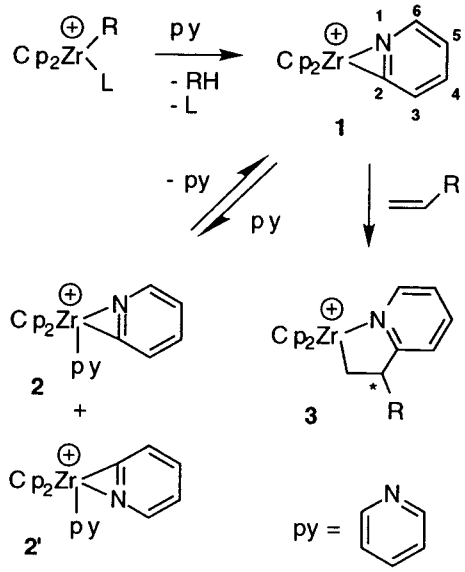

In a recent communication we reported that the chiral zirconocene η^2-pyridyl species *rac*-(EBI)Zr(η^2-6-R-pyrid-2-yl)$^+$ (EBI = ethylenebis(indenyl)) and *rac*-(EBTHI)-Zr(η^2-6-R-pyrid-2-yl)$^+$ (EBTHI = ethylenebis(tetrahydroindenyl)) insert α-olefins stereoselectively.[3,4] Here we describe a more detailed study of the propene

[⊗] Abstract published in *Advance ACS Abstracts,* November 15, 1997.

(1) For reviews concerning the chemistry of cationic group 4 metallocene complexes see: (a) Guram, A. S.; Jordan, R. F. In *Comprehensive Organometallic Chemistry II*; Abel, E. W., Stone, F. G. A., Wilkinson, G., Eds.; Elsevier: Oxford, U.K., 1995; Vol. 4, p 589. (b) Bochmann, M. *J. Chem. Soc., Dalton Trans.* **1996**, 255. (c) Horton, A. D. *Trends Polym. Sci.* **1994**, *2*, 158. (d) Marks, T. J. *Acc. Chem. Res.* **1992**, *25*, 57. (e) Jordan, R. F. *Adv. Organomet. Chem.* **1991**, *32*, 325. (f) Jordan, R. F.; Bradley, P. K.; Lapointe, R. E.; Taylor, D. F. *New J. Chem.* **1990**, *14*, 505.

(2) (a) Jordan, R. F.; Taylor, D. F. *J. Am. Chem. Soc.* **1989**, *111*, 778. (b) Jordan, R. F.; Taylor, D. F.; Baenziger, N. C. *Organometallics* **1990**, *9*, 1546. (c) Jordan, R. F.; Guram, A. S. *Organometallics* **1990**, *9*, 2116. (d) Guram, A. S.; Jordan, R. F. *Organometallics* **1990**, *9*, 2190. (e) Guram, A. S.; Jordan, R. F.; Taylor, D. F. *J. Am. Chem. Soc.* **1991**, *113*, 1833. (f) Guram, A. S.; Jordan, R. F. *Organometallics* **1991**, *10*, 3470. (g) Guram, A. S.; Swenson, D. C.; Jordan, R. F. *J. Am. Chem. Soc.* **1992**, *114*, 8991. (h) Guram, A. S.; Jordan, R. F. *J. Org. Chem.* **1992**, *57*, 5994. (i) Guram, A. S.; Jordan, R. F. *J. Org. Chem.* **1993**, *58*, 5995.

(3) Rodewald, S.; Jordan, R. F. *J. Am. Chem. Soc.* **1994**, *116*, 4491.

S0276-7333(97)00750-4 CCC: $14.00

insertion reactions of a series of *rac*-(EBI)Zr(η^2-pyridyl)$^+$ species containing substituted η^2-pyridyl groups. The specific objectives of this work were to determine the influence of the η^2-pyridyl substituents on the insertion stereoselectivity and to develop a detailed understanding of the stereocontrol mechanism.

Results and Discussion

In previous papers in this series, many achiral $Cp_2Zr(\eta^2\text{-pyridyl})^+$ complexes and $Cp_2Zr\{\eta^2(C,N)\text{-}CH_2CHR\text{-(pyridyl)}\}^+$ insertion products have been isolated and characterized, and X-ray crystallographic studies on key compounds have been reported.[2] In the present work, most reactions were performed on an NMR scale, and product yields and ratios were determined by ^{1}H NMR spectroscopy. Regio-and stereochemical assignments were made by 1D and 2D NMR (COSY, NOESY, HMQC, HMBC) techniques and by ^{1}H NMR and GC−MS analysis of hydrolysis products.[5,6]

Generation of *rac*-(EBI)Zr(η^2-pyridyl)$^+$ Species. The reaction of *rac*-(EBI)$ZrMe_2$ with $B(C_6F_5)_3$ in CH_2Cl_2 at 23 °C quantitatively generates [*rac*-(EBI)ZrMe]-[$MeB(C_6F_5)_3$] (**4**; Scheme 2), which was characterized by ^{1}H NMR and used *in situ*.[7] The ^{1}H NMR spectrum of **4** contains four doublets for the indenyl C_5 ring hydrogens, which is characteristic of a C_1-symmetric structure. The *Me*$B(C_6F_5)_3^-$ signal appears as a broad singlet at high field (δ −0.57), indicating that the anion is coordinated to the metal center; for comparison, the free anion resonance appears at ca. δ 0.5.[7]

Complex **4** reacts quantitatively in CH_2Cl_2 (23 °C, <20 min) with the appropriate pyridine to yield CH_4 and the chiral η^2-pyridyl complexes [*rac*-(EBI)Zr(η^2-pyridyl)]-[$MeB(C_6F_5)_3$] (**5a**−**f**; Scheme 2). Structural assignments for **5a**−**f** are based on NMR data, which are similar to data for achiral analogs which were characterized previously.[2] The ^{1}H NMR spectra of **5a**−**f** each contain four doublets for the indenyl C_5 ring hydrogens, as expected for C_1-symmetric structures. The presence of a metalated pyridyl group is evident from the absence of Zr*Me* resonances and from the patterns observed for η^2-pyridyl resonances. For free and coordinated pyridines, the ortho hydrogen resonances appear at low field (δ 8.3−8.7).[8] For **5a**,**b**,**d**,**e**, the characteristic low-field pyridine ortho hydrogen resonance is absent, and for **5c**,**f** the ortho hydrogen resonance (δ 8.41 and 8.37, respectively) integrates for one hydrogen. In the case of **5a**, the ortho C−H activation and η^2-pyridyl coordination were confirmed by the $^{13}C\{^1H\}$ NMR spectrum, which exhibits a low-field Zr−*C* resonance (δ 201.2) characteristic of the ipso carbon of the three-membered Zr−C−N ring in these systems.[2a,c] Additionally, the *Me*$B(C_6F_5)_3^-$ ^{1}H NMR signal for **5a**−**f** appears at δ 0.53, which indicates that the anion is not coordinated. Anion coordination would be expected if the pyridyl ligands in **5a**−**f** were bonded in an η^1 mode.

Complexes **5a**−**f** were generated and used *in situ* but not isolated. However, the closely related η^2-pyridyl pyridine complexes [*rac*-(EBI)Zr(η^2-6-methylpyrid-2-yl)-(2-methylpyridine)][BPh_4] and [*rac*-(EBI)Zr(η^2-6-phenylpyrid-2-yl)(2-phenylpyridine)][$B(C_6F_5)_4$] were isolated from the reactions of *rac*-(EBI)$ZrMe_2$ with HNR_3^+ reagents in the presence of an excess of the appropriate pyridine.

Scheme 2

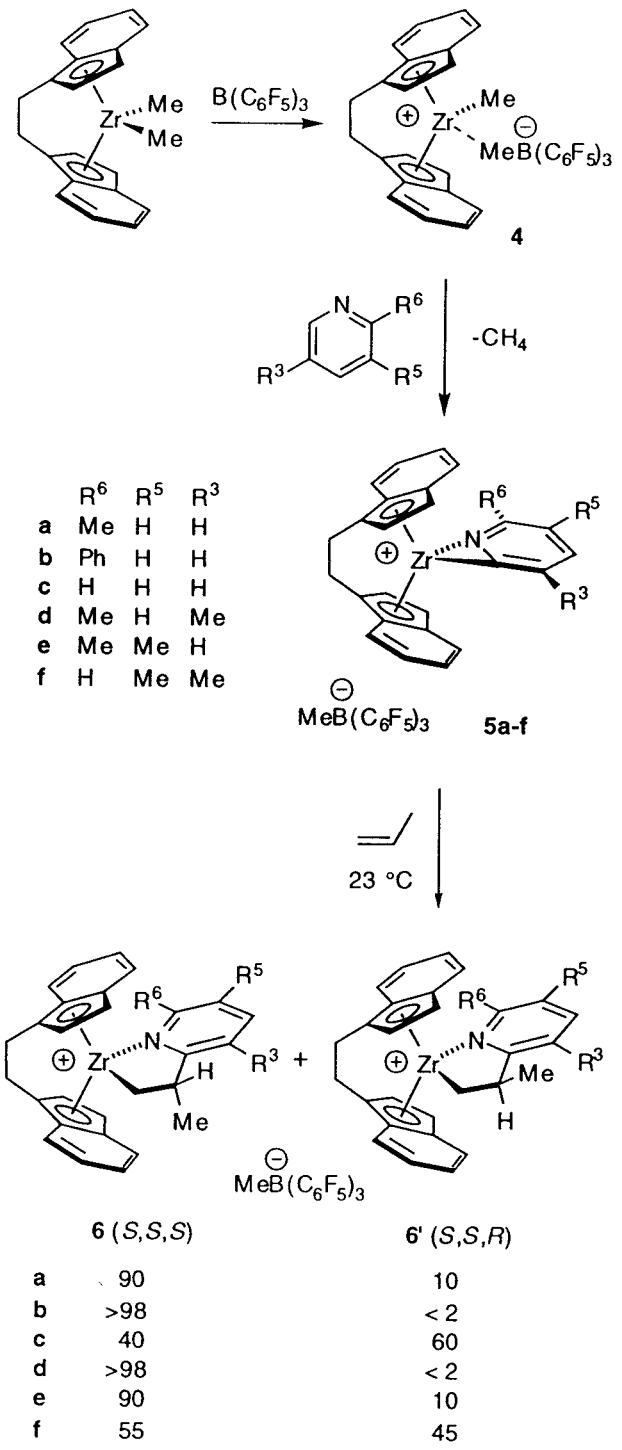

	R6	R5	R3
a	Me	H	H
b	Ph	H	H
c	H	H	H
d	Me	H	Me
e	Me	Me	H
f	H	Me	Me

	6 (*S*,*S*,*S*)	6' (*S*,*S*,*R*)
a	90	10
b	>98	< 2
c	40	60
d	>98	< 2
e	90	10
f	55	45

(4) For recent reviews concerning other applications of chiral zirconocene complexes, see: (a) Hoveyda, A. H.; Morken, J. P. *Angew. Chem., Int. Ed. Engl.* **1996**, *35*, 1263. (b) Brintzinger, H. H.; Fischer, D.; Mülhaupt, R.; Rieger, B.; Waymouth, R. M. *Angew. Chem., Int. Ed. Engl.* **1995**, *34*, 1143. (c) Halterman, R. L. *Chem. Rev.* **1992**, *92*, 965.

(5) HMQC: Bax, A.; Griffey, R. H.; Hawkins, B. L. *J. Magn. Reson.* **1983**, *55*, 301.

(6) HMBC: Bax, A.; Summers, M. F. *J. Am. Chem. Soc.* **1986**, *108*, 2093.

(7) For use of $B(C_6F_5)_3$ in metallocene cation generation see: (a) Yang, X.; Stern, C. L.; Marks, T. J. *J. Am. Chem. Soc.* **1994**, *116*, 10015. (b) Deck, P. A.; Marks, T. J. *J. Am. Chem. Soc.* **1995**, *117*, 6128. (c) Giardello, M. A.; Eisen, M. S.; Stern, C. L.; Marks, T. J. *J. Am. Chem. Soc.* **1995**, *117*, 12114. (d) Chen, Y.-X.; Stern, C. L.; Yang, S.; Marks, T. J. *J. Am. Chem. Soc.* **1996**, *118*, 12451.

(8) ^{1}H NMR chemical shifts for the ortho-H resonances of relevant pyridines (CD_2Cl_2): 2-methylpyridine, 2,5-dimethylpyridine: δ 8.55; pyridine, 3,5-dimethylpyridine: δ 8.50; 2-phenylpyridine, δ 8.70.

Reaction of *rac*-(EBI)Zr(η^2-pyridyl)$^+$ Species with Propene. As illustrated in Scheme 2, η^2-pyridyl complexes **5a**−**f** react regiospecifically with propene at 23 °C to yield the 1,2-insertion products **6a**−**f**/**6a′**−**f′**, as mixtures of diastereomers which differ in the relative stereochemistry of the (EBI)Zr metallocene and C_β of the metallacycle. The configurations of **6a**−**f** and **6a′**−**f′** may be denoted by the descriptors *S*,*S*,*S* and *S*,*S*,*R*, respectively, where the first two entries denote the configuration of the EBI bridgehead carbons and the third denotes that of C_β; the configurations of the enantiomers, which are not shown in Scheme 2, are *R*,*R*,*R* and *R*,*R*,*S*.[9]

The stereoselectivity of the reaction of **5a**−**f** with propene is very sensitive to the substituents on the η^2-pyridyl group. High stereoselectivity for the *S*,*S*,*S* (*R*,*R*,*R*) product **6** is observed for **5a**,**b**,**d**,**e**, in which a Me or a Ph group is present at the pyridyl 6-position (R^6), while poor stereoselectivity is observed for **5c** and **5f**, which lack a pyridyl 6-substituent. Interestingly, the *S*,*S*,*R* (*R*,*R*,*S*) product **6c′** is slightly favored for **5c**. The de = 80% observed for **5a** is improved to >96% (no detectable *S*,*S*,*R* product) by replacement of the 6-Me group by a Ph group (**5b**) or by incorporation of an additional Me substituent (R^3) at the 3-position of the pyridyl ring (**5d**). However, the results for **5e** show that incorporation of an additional Me substituent at the 5-position (R^5) has no effect on the stereoselectivity.

The rate of the reaction of **5a**−**f** with propene is also sensitive to the η^2-pyridyl substituent pattern. Complexes **5a**,**b**,**d**,**e**, which contain a pyridyl 6-substituent, react with excess propene (10 equiv) in CH_2Cl_2 at 23 °C to yield the corresponding insertion products **6a**/**6a′**, **6b**, **6d**, and **6e**/**6e′** quantitatively in less than 15 min. In contrast, complexes **5c** and **5f**, which lack a pyridyl 6-substituent, are much less reactive with propene, and complete conversion to **6c**/**6c′** and **6f**/**6f′** requires 5 days for **5c** and 8 days for **5f** at 23 °C. NMR experiments using *m*-xylene as an internal standard confirm that no species other than **6**/**6′** are formed in those reactions and that the NMR yields are >98%.

Although several attempts to isolate **6**/**6′** were unsuccessful using $MeB(C_6F_5)_3^-$ as a counterion, we were able to isolate **6a**/**6a′** as the BPh_4^- salt. Thus, the reaction of [*rac*-(EBI)Zr(η^2-6-methylpyrid-2-yl)(2-methylpyridine)]-[BPh_4] (mixture of N-inside and N-outside isomers) with 10 equiv of propene in CH_2Cl_2 at 23 °C yields [**6a**/**6a′**]-[BPh_4] in 91% isolated yield and a 90/10 **6a**/**6a′** ratio (Scheme 3).[10]

Determination of Regiochemistry of 6/6′. The regiochemistry of **6**/**6′** was established by 1D and 2D NMR studies and further confirmed for **6d**, **6e**/**6e′**, and **6f**/**6f′** by GC−MS and ^{1}H NMR analysis of the hydrolysis products. The $^{13}C\{^1H\}$ NMR and 2D $^1H-^{13}C$ HMQC spectra of **6a**−**f** are similar to those obtained for [*rac*-(EBI)Zr{η^2(*C*,*N*)-CH_2CHBu(6-methylpyridyl)}][BPh_4] (**7**; Scheme 3), which was structurally characterized by

Scheme 3

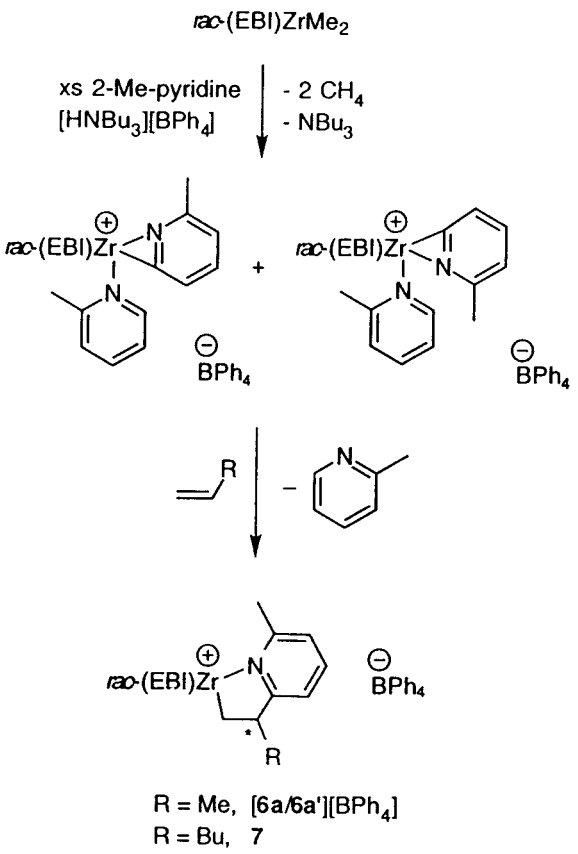

X-ray crystallography.[3,11] The Zr*C*H_2 and ZrCH_2*C*HR ^{13}C NMR resonances of **7** appear at δ 62.8 and 45.2, respectively. The $^{13}C\{^1H\}$ spectra of **6a**/**6a′**, **6b**, **6c**/**6c′**, **6d**, **6e**/**6e′**, and **6f**/**6f′** each contain a characteristic signal at δ 60−66, which is assigned to the metallacycle α-carbon, and one at δ 40−48, which is assigned to the metallacycle β-carbon. 2D $^1H-^{13}C$ HMQC data for these compounds show that in each case C_α is a methylene carbon and C_β is a methine carbon, establishing that these complexes are 1,2-insertion products.

Hydrolysis of **6d**, **6e**/**6e′**, and **6f**/**6f′** yields isopropylpyridines **8d**−**f** as single isomers (eq 1). In each case,

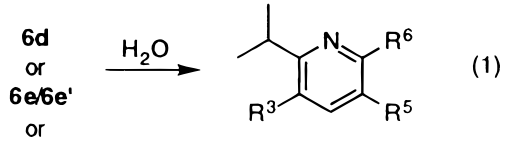

	R^6	R^5	R^3
8d	Me	H	Me
8e	Me	Me	H
8f	H	Me	Me

GC−MS analysis of the hydrolysis products shows that the single pyridine product which is formed exhibits a parent ion peak at *m*/*z* = 149. Parent ions derived from pyridines containing *n*-propyl or higher substituents in the 2- and/or 6-positions normally undergo McLafferty rearrangement with the elimination of olefin.[12] The mass spectra of **8d**−**f** do not exhibit peaks at *m*/*z* 121

(9) (a) Cahn, R. S.; Ingold, C. K.; Prelog, V. *Angew. Chem., Int. Ed. Engl.* **1966**, *5*, 385. (b) Brunner, H. *Top. Stereochem.* **1989**, *18*, 129.

(10) The observation of identical stereoselectivity for propene insertion of **5a** and [*rac*-(EBI)Zr(η^2-6-methylpyrid-2-yl)(2-methylpyridine)]-[BPh_4] shows that neither the presence of excess pyridine nor the counterion influence stereoselectivity in these reactions. Similarly, the same stereoselectivity is observed for propene insertion of **5b** and [*rac*-(EBI)Zr(η^2-6-phenylpyrid-2-yl)(2-phenylpyridine)][$MeB(C_6F_5)_3$].

(11) Bowen, D. E.; Rodewald, S. R.; Swenson, D. C.; Jordan, R. F., submitted for publication.

(12) Micetich, R. G. In *Pyridine and its Derivatives*; Abramovich, R. A., Ed.; Wiley: New York, 1974; Vol. 2, p 305.

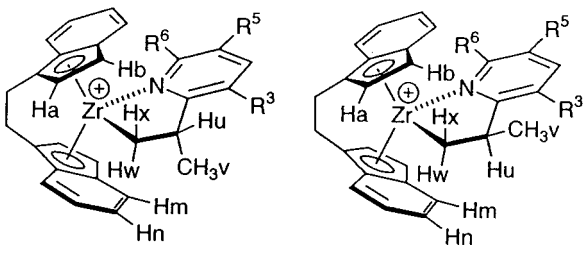

Figure 1. Atom-labeling scheme for **6** and **6′**.

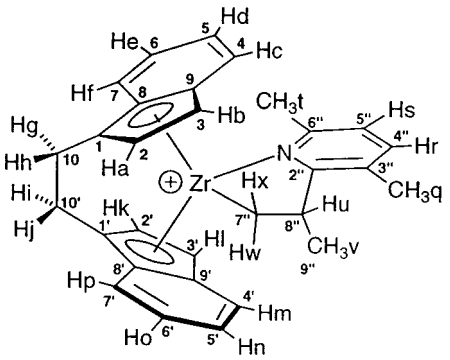

Figure 2. Atom-labeling scheme for **6d**.

(M − ethylene), indicating that no McLafferty rearrangement occurs. However, these spectra do contain intense peaks at *m*/*z* 134 (M − Me) resulting from *β*-cleavage, which is consistent with the presence of an isopropyl group.[13] The ^{1}H NMR spectra of **8d**−**f** each contain a septet at *δ* 3.0−3.2 (1H) and a doublet at *δ* 1.1−1.3 (6H), which are characteristic of an isopropyl group.[14]

Determination of Stereochemistry of 6/6′. The ^{1}H NMR spectra of **6**/**6′** were completely assigned using general chemical shift trends and a combination of 1D and 2D NMR spectra. The stereochemistry of **6**/**6′** was then established by NOESY experiments. Labeling schemes are shown in Figure 1. The NOESY spectra of **6a**−**f** all show a correlation between H_u and H_b, placing H_u in the vicinity of the "top" C_5 indenyl ring (Figure 1). NOESY correlations are also observed between H_v and H_m and H_n, placing H_v in the vicinity of the "bottom" C_6 indenyl ring. These correlations establish the stereochemistry of **6a**−**f**. The same approach was used to determine the stereochemistry of the diastereomers **6a′**,**c′**,**e′**,**f′**.

Detailed Regio- and Stereochemical Assignment for 6d. To illustrate the general strategies for assignment of regio- and stereochemistry of **6**/**6′** discussed in the preceding sections, a detailed discussion of the analysis of one case, **6d**, is presented in this section.

^{1}H and ^{13}C NMR data and listings of key COSY and NOESY correlations for **6d** are included in the Experimental Section. A full labeling scheme for **6d** is given in Figure 2. For clarity, only the *S*,*S*,*S* configuration is shown. Hydrogen atoms are denoted by letters and carbon atoms by numbers and primes. The primes denote the ligand on which the carbon resides (no prime, top indenyl; one prime, bottom indenyl; double prime, pyridyl ring).

In EBI complexes of this type, the indenyl ^{1}H NMR resonances can be assigned directly by their characteristic coupling patterns. The hydrogens on the five-membered (C_5) indenyl rings (H_a, H_b, H_k, H_l) appear as doublets with ^3J = 3.0−3.2 Hz. The hydrogens at the 2 and 2′ positions, H_a and H_k, can be identified by their NOESY correlations with the hydrogens on the ethylene bridge. A NOESY correlation between H_a and H_x indicates that H_a is on the $-CH_2CHMe$ side of the complex and thus permits the assignment of H_a (*δ* 5.82, d, ^3J = 3.2 Hz). Once H_a is assigned, H_k can be assigned (*δ* 6.59, d, ^3J = 3.1 Hz). COSY correlations between H_a and H_b and between H_k and H_l allow the assignment of H_b (*δ* 6.82, d, ^3J = 3.2 Hz) and H_l (*δ* 6.48−6.52).[15] The indenyl benzo hydrogens which are ortho to the C_5 rings (H_c, H_f, H_m, H_p) appear as doublets with ^3J = 8−9 Hz, while those meta to the C_5 rings (H_d, H_e, H_n, H_o) appear as doublets of doublets with ^3J = 6.5−8.5 Hz. H_c (*δ* 6.48−6.52) is assigned by its NOESY correlation with H_b. COSY correlations then allow the assignment of H_d (*δ* 6.76, dd, ^3J = 7.6, 6.6 Hz), H_e (*δ* 7.20, dd, ^3J = 8.3, 6.6 Hz), and then H_f (*δ* 7.51, d, ^3J = 8.6 Hz). H_m−H_p can be assigned in a similar manner.

The ^{1}H NMR spectrum of **6d** contains two singlets at *δ* 0.99 and 2.37 (each 3H) for the pyridyl methyl groups. The *δ* 0.99 resonance exhibits NOESY correlations with H_c, H_d, H_k, and H_l and is therefore assigned to H_t. The high-field chemical shift of H_t (vs *δ* 2.4−2.6 for 2-methylpyridines) is due to the ring current effect of the top C_6 indenyl ring. Once H_t is assigned, the *δ* 2.37 resonance may be assigned to H_q. H_r (*δ* 7.57, ^3J = 7.8 Hz) is assigned by its NOESY correlation with H_q. A COSY correlation between H_r and H_s permits the assignment of H_s (*δ* 6.87, ^3J = 7.8 Hz). This assignment is confirmed by a NOESY correlation between H_s and H_t.

The ^{1}H NMR spectrum of **6d** contains two coupled doublets of doublets at *δ* 1.55 (^2J = 13.8 Hz, ^3J = 4.6 Hz) and *δ* −1.21 (^2J = 13.8 Hz, ^3J = 9.6 Hz), each integrating for 1H. The 2D ^{1}H−^{13}C HMQC spectrum reveals that these two hydrogens correlate to the Zr−*C*H_2 resonance at *δ* 64.4. Thus, these two resonances correspond to H_x and H_w. The *δ* 1.55 resonance exhibits NOESY correlations with H_a and H_b and is thus assigned to H_x, the hydrogen which is close to the C_5 indenyl ring. The *δ* −1.21 resonance is then assigned to H_w. The high-field shift for H_w is consistent with the proximity of this hydrogen to the indenyl C_6 ring. COSY correlations between H_x and H_u and between H_w and H_u permit the assignment of H_u (*δ* 3.51−3.66, m). A COSY correlation between H_u and H_v allows the assignment of H_v. The assignment of H_u is also confirmed by the 2D ^{1}H−^{13}C HMQC spectrum, in which H_u correlates to the ZrCH_2*C*HR (*C*$_\beta$) resonance at *δ* 40.2. This establishes the 1,2-insertion regiochemistry of **6d**.

The configuration of C_β ($C_{8''}$) in **6d** was established by NOESY experiments. NOESY correlations between H_u and H_b and between H_v and H_m and H_n show that H_u is close to the C_5 indenyl ring and H_v is close to the C_6 indenyl ring. These results establish that **6d** is the *S*,*S*,*S* (*R*,*R*,*R*) diastereomer. This stereochemistry is

(13) Silverstein, R. M.; Bassler, G. C.; Morril, T. C. *Spectrometric Identification of Organic Compounds*, 5th ed.; Wiley: New York, 1991; p 15.

(14) Similar pyridines have been reported. (a) Vernaudon, P.; Rajohrison, H. G.; Roussel, C. *Bull. Soc. Chim. Fr.* **1987**, *1*, 205. (b) Vymetal, J.; Koksochem, V. U.; Zavody, U.; Mezirici, V. *Chem. Prum.* **1979**, *29*, 354.

(15) The ^{1}H NMR resonances of H_c and H_l are overlapped for **6d**.

Table 1. Time Dependence of Product Distribution from the Reaction of 5d and Propene (80 °C)[a]

time (h)	6d	6d′	6d″
0.5	100		
2.5	65	14	21
5	57	16	27
15	18	18	64
48	14	14	64

[a] Values are percentages of the total EBI species, as measured versus an internal standard (*m*-xylene).

Scheme 4

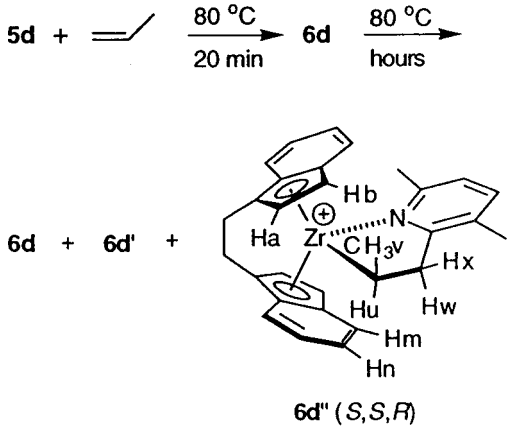

confirmed by NOESY correlations between H_w and H_v, H_m, and H_n, and between H_x and H_a.

Reaction of 5a and 5e with Propene at Low Temperature. To probe whether the **6**/**6′** product ratios obtained at 23 °C are kinetic or thermodynamic ratios, we investigated the reactions of **5a** and **5e** with propene at low temperature.[16] A solution of **5a** or **5e** in CD_2Cl_2 was frozen at −196 °C, excess propene was added, and the reaction mixture was carefully warmed to −88 °C and monitored by ^{1}H NMR at that temperature. Complexes **5a** and **5e** react quantitatively with propene within 1 h at −88 °C to afford the insertion products, with **6a**/**6a′** = **6e**/**6e′** = 90/10. Thus, for both cases the regio- and stereoselectivity at −88 °C is identical with that observed at 23 °C.

Reaction of 5d with Propene at High Temperature. To determine the thermodynamic **6**/**6′** ratios, we investigated the reactions of **5a**−**f** with propene at high temperature. The reaction of **5d** with propene at 80 °C in C_6D_5Cl was monitored by ^{1}H NMR using *m*-xylene as an internal standard. As summarized in Table 1 and Scheme 4, this reaction is complete in less than 30 min and yields **6d** quantitatively. However, when the solution is maintained at 80 °C, the amount of **6d** decreases and two new species, **6d′** (the *S*,*S*,*R*/*R*,*R*,*S* diastereomer of **6d**) and **6d″** (the 2,1 regioisomer of **6d**), are formed. After 15 h at 80 °C, the major species present is **6d″**, and the relative amounts of **6d**, **6d′**, and **6d″** remain constant, indicating that the system has reached equilibrium. The use of an internal standard enabled detection of 8% decomposition after 2 days at 80 °C. Decomposition products include (EBI)H_2 (4%), which probably results from trace hydrolysis, and *rac*-(EBI)-$ZrCl_2$ (4%), which probably results from reaction of **6d**, **6d′**, or **6d″** with the solvent.[17]

Complexes **6d′** and **6d″** were identified by 1D and 2D NMR studies of the thermodynamic **6d**/**6d′**/**6d″** mixture and by ^{1}H NMR and GC-MS analyses of the hydrolysis product of this mixture. The NMR data for **6d′** are similar to those observed for **6a′**,**c′**,**e′**,**f′** and show that this species is the *S*,*S*,*R* (*R*,*R*,*S*) diastereomer. The 2D NOESY spectrum of **6d′** contains correlations between H_v and H_b and between H_u and H_m and H_n (see Figure 1 for labeling), showing that H_v is close to the C_5 indenyl ring and H_u is close to the C_6 indenyl ring and establishing the configuration at C_β.

The ^{13}C{^{1}H} NMR spectrum of **6d″** contains signals at δ 66.7 and 41.1, which are assigned to the Zr−*C* and Zr−C−*C* carbons, respectively. 2D HMQC data show that C_α is a methine carbon and C_β is a methylene carbon, thus establishing the 2,1-regiochemistry of **6d″**. The ^{1}H NMR spectrum of **6d″** contains a doublet at δ 0.86 (3H), which is assigned to the Zr−CH*Me*− hydrogens (H_v; see Scheme 4 for labeling). The Zr−C*H*Me− resonance (H_u) can be assigned by its correlations with C_α in the HMQC spectrum and with H_v in the NOESY and COSY spectra. The Zr−CHMeCH_2− hydrogens H_x and H_w are assigned by their HMQC correlations with C_β and by their respective NOESY correlations with H_v and H_u. The NOESY spectrum of **6d″** exhibits correlations between H_v and the C_5 ring hydrogens H_a and H_b and between H_x and H_b and thus establishes the stereochemistry as *S*,*S*,*R* (*R*,*R*,*S*), where the third entry denotes the configuration of C_α.

Hydrolysis of the thermodynamic **6d**/**6d′**/**6d″** mixture yields a 28/64 mixture of pyridines **8d** and **8d″**, as determined by ^{1}H NMR and GC−MS analysis (eq 2).

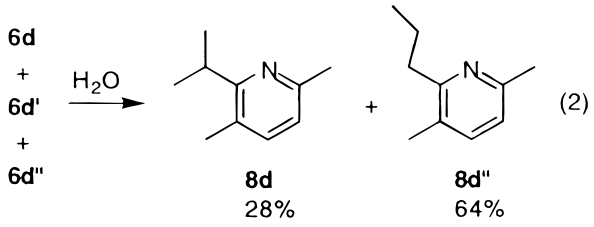

(2)

The ^{1}H NMR and MS data establish that **8d** contains an isopropyl substituent while **8d″** contains an *n*-propyl group. The minor product **8d** results from hydrolysis of **6d** and **6d′**, while the major product **8d″** results from hydrolysis of **6d″**.

The most likely mechanism for the isomerization of **6d** to **6d′**/**6d″** is deinsertion of propene to form **5d**, followed by reinsertion with the opposite stereochemistry to yield **6d′** or with the opposite regiochemistry to yield **6d″**, as illustrated in Scheme 5. Similar reactivity was observed previously for achiral analogs; e.g., Cp_2-Zr{η^2(*C*,*N*)-CH_2CHMe(6-phenylpyrid-2-yl)}$^+$ undergoes propene deinsertion at 80 °C in the presence of allyltrimethylsilane.[2f] Consistent with Scheme 5, thermolysis of pure **6d** (formed at 23 °C) at 80 °C for 2 days yields the thermodynamic **6d**/**6d′**/**6d″** mixture. However, **6d** does not isomerize to **6d′** and **6d″** at 23 °C.

The observations discussed in this section establish that **6d** is the kinetic product of the reaction of **5d** with

(16) The propene reactions of the other pyridyl complexes were not investigated at low temperature because (i) **5c** and **5f** react slowly with propene at room temperature, making these systems inconvenient for low-temperature experiments, and (ii) the propene insertion reactions of **5b** and **5d** are >98% regio- and stereoselective at room temperature.

(17) For comparison, the reaction of **5d** with propene in CD_2Cl_2 at 80 °C yields 80% *rac*-(EBI)$ZrCl_2$.

Scheme 5

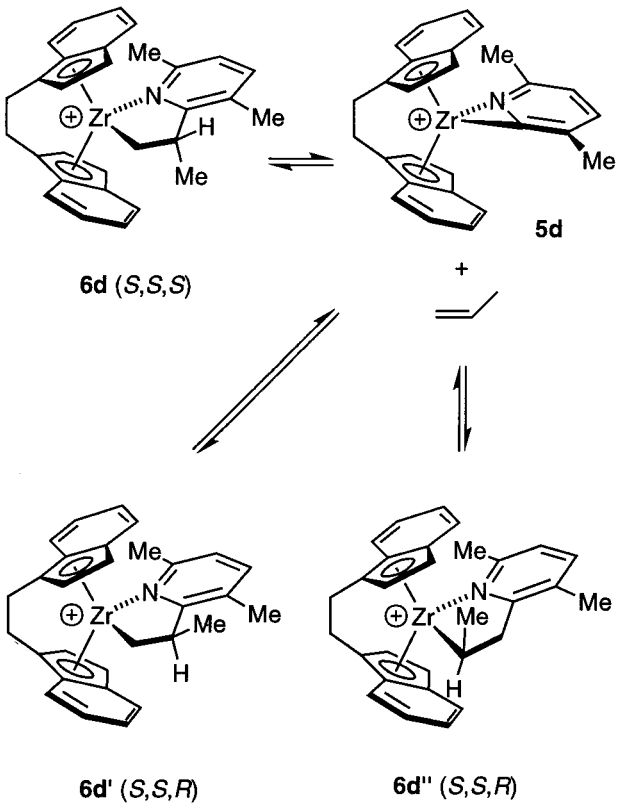

Scheme 6

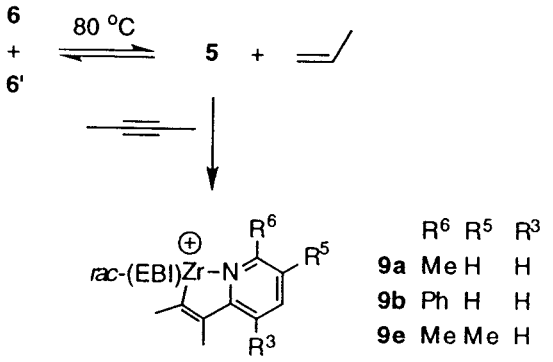

propene and that **6d** isomerizes to a mixture of **6d**, diastereomer **6d′**, and regioisomer **6d″** at 80 °C.

Reaction of 5a−c,e,f with Propene at High Temperature. The reaction of **5a** with excess propene (1 atm) at 80 °C in C_6D_5Cl for 30 min quantitatively yields a 90/10 mixture of **6a**/**6a′**; this is the same product ratio observed at 23 °C. The **6a**/**6a′** ratio does not change after 2 days at 80 °C. To determine whether **6a** and **6a′** can undergo propene deinsertion at 80 °C, which is required for the **6a**/**6a′** isomerization, 2-butyne was added to the reaction mixture. It was anticipated that any **5a** generated by deinsertion of **6a** and **6a′** would be trapped by 2-butyne, yielding the stable metallacycle *rac*-(EBI)Zr{η^2(*C*,*N*)-CMe=CMe(6-methylpyrid-2-yl)}$^+$ (**9a**; Scheme 6).[2b] Addition of 2-butyne to the **6a**/**6a′** mixture at 23 °C does not result in a detectable reaction, indicating that **6a**/**6a′** do not deinsert propene at this temperature. However, heating the **6a**/**6a′**/2-butyne mixture at 80 °C for 8 h results in quantitative formation of **9a** and propene, indicating that **6a** and **6a′** do undergo deinsertion under these conditions. These observations establish that the 90/10 **6a**/**6a′** product ratio obtained from the reaction of **5a** and propene at 23 °C is the kinetic ratio and that the thermodynamic **6a**/**6a′** ratio is coincidentally identical with this value.

Table 2. Kinetic (23 °C) and Thermodynamic (80 °C) Product Ratios for the Reaction of 5a−f with Propene

					thermodynamic ratio[b]	
reactant	R^6	R^5	R^3	kinetic ratio[a] **6**/**6′**	**6**/**6′**	(**6** + **6′**)/**6″**
5a	Me	H	H	90/10	90/10	
5b	Ph	H	H	98/2	98/2	
5c	H	H	H	40/60	50/50	
5d	Me	H	Me	98/2	50/50	28/64
5e	Me	Me	H	90/10	90/10	
5f	H	Me	Me	55/45	50/50	

[a] 23 °C. [b] 80 °C.

Compound **9a** was generated independently by the reaction of 2-butyne and **5a** at 23 °C and characterized by NMR. The NMR data for **9a** are very similar to data for the achiral analog $Cp_2Zr\{\eta^2(C,N)$-CMe=CMe-(6-methylpyrid-2-yl)$\}^+$ (**10**), which was previously characterized.[2b] The ^1H and $^{13}C\{^1H\}$ NMR spectra of **9a** contain resonances for two inequivalent indenyl ligands, expected for a cyclic structure. The ^1H NMR spectrum contains resonances for the two alkenyl Me groups (δ 1.29 and 1.73) and the pyridyl Me group (δ 1.39). The $^{13}C\{^1H\}$ spectrum contains a low-field resonance (δ 214.2) characteristic of the Zr−*C*Me= alkenyl carbon. The identity of **9a** was confirmed by hydrolysis, which yields **11a** (eq 3).

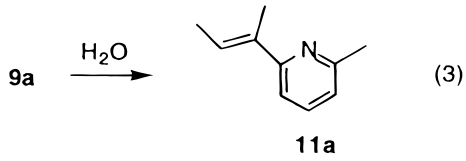

(3)

The propene insertion stereoselectivity of **5b**,**c**,**e**,**f** was studied at 80 °C using the same approach as described for **5a**. The **6b**/**6b′** and **6e**/**6e′** ratios formed from propene insertion of **5b**,**e** at 23 °C do not change upon heating the product mixture to 80 °C, and propene deinsertion was shown to occur at 80 °C (and not at 23 °C) using the 2-butyne insertion reaction as a probe (Scheme 6). In contrast, the 40/60 **6c**/**6c′** and 55/45 **6f**/**6f′** mixtures formed from propene insertion of **5c**,**f** at 23 °C isomerize to 50/50 **6c**/**6c′** and **6f**/**6f′** mixtures after 2 h at 80 °C.

The kinetic (23 °C) and thermodynamic (80 °C) **6**/**6′** product ratios for **6a**−**f** are summarized in Table 2.

Molecular Modeling Studies. To probe the influence of the pyridyl substituents on the stereoselectivity of propene insertion of *rac*-(EBI)Zr(η^2-pyridyl)$^+$ species, molecular modeling calculations were performed for several model *rac*-(EBI)Zr(η^2-pyridyl)(propene)$^+$ propene adducts and several *rac*-(EBI)Zr{η^2(*C*,*N*)-CH_2CHMe-(pyrid-2-yl)$\}^+$ insertion products. The structures of these compounds were studied by molecular dynamics/mechanics methods using Rappé's universal force field (UFF) as implemented in the Cerius[2] (Molecular Simulations) software package.[18] Computational details are provided in the Experimental Section. In each case, the

(18) (a) Rappé, A. K.; Casewit, C. J.; Colwell, K. S.; Goddard, W. A., III; Skiff, W. M. *J. Am. Chem. Soc.* **1992**, *114*, 10024. (b) Rappé, A. K.; Colwell, K. S.; Casewit, C. J. *Inorg. Chem.* **1993**, *32*, 3438.

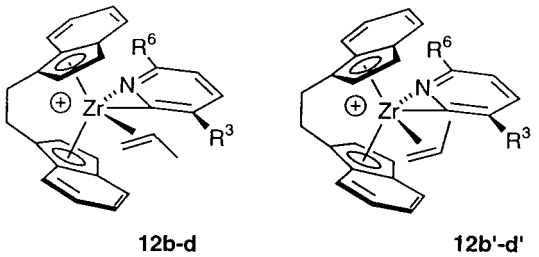

Figure 3. Diastereomeric propene adducts **12** and **12′** (**b**, $R^3 = H$, $R^6 = Ph$; **c**, $R^3 = R^6 = H$; **d**, $R^3 = R^6 = Me$).

structure was built, minimized, and then subjected to 10 5 ps runs of molecular dynamics, leading to 10 high-energy structures, which were subsequently minimized. For each system, the energies of the 10 minimized structures were within a 0−3 kcal/mol range. For most systems, two (EBI)Zr conformations, "indenyl-forward" and "indenyl-back", which differ in energy by 0−3 kcal/mol were observed. This is consistent with NMR and structural data for *rac*-(EBI)ZrX_2 complexes, which show that the indenyl-forward and indenyl-back conformations generally are very similar in energy.[19] No general trends were observed concerning the relative stabilities of the two conformations. The most stable of the 10 minimized structures for each system was used for structural comparisons.

(i) Comparison of *rac*-(EBI)Zr(η^2-pyridyl)(propene)$^+$ Species. It is presumed that propene insertion reactions of *rac*-(EBI)Zr(η^2-pyridyl)$^+$ species proceed via intermediate *rac*-(EBI)Zr(η^2-pyridyl)(propene)$^+$ adducts. As shown in Figure 3, two diastereomers which differ in the propene enantioface which is coordinated are possible for these species: **12**, which leads to the *S*,*S*,*S* (*R*,*R*,*R*) insertion product **6**, and **12′**, which leads to the *S*,*S*,*R* (*R*,*R*,*S*) product **6′**. The structures of three pairs of diastereomers, **12b**/**12b′**, **12c**/**12c′**, and **12**/**12d′**, were investigated. These examples were chosen for study because the corresponding base-free η^2-pyridyl species **5b** and **5d** insert propene with high stereoselectivity for the *S*,*S*,*S* (*R*,*R*,*R*) products **6b** and **6d**, while **5c** exhibits low and opposite stereoselectivity.

One challenging aspect of modeling **12**/**12′** is treatment of the Zr−propene interaction. Olefin complexes of d^0 metals are extremely rare, and little experimental information concerning the metal−olefin bonding in such systems is available. However, we recently determined the structures of two chelated Zr(IV) olefin complexes, $Cp_2Zr(OCMe_2CH_2CH_2CH{=}CH_2)^+$ and *rac*-(EBI)$Zr(OCMe_2CH_2CH_2CH{=}CH_2)^+$.[20,21] In both cases, unsymmetrical bonding with long Zr−CH_2= distances (2.63−2.68 Å) and very long Zr−CHR= distances (2.82−2.89 Å) was observed. Furthermore, the ^1H and ^{13}C NMR data for the olefin groups of $Cp_2Zr(OCMe_2CH_2CH_2CH{=}CH_2)^+$ and $Cp_2Zr(OCMe_2CH_2CH_2CH_2CH{=}CH_2)^+$ are nearly identical, which argues that the metal−olefin interaction is very similar in both species and is not strongly influenced by constraints imposed by the linking group. Thus, these species are reasonable structural models for nonchelated $Cp_2Zr(X)(propene)^+$ species, and the structural data for *rac*-(EBI)$Zr(OCMe_2CH_2CH_2CH{=}CH_2)^+$ were used in our computations on **12**/**12′**. The Zr−C−N bond distances and angles associated with the Zr(η^2-pyridyl) unit were constrained to be equal to values found for $Cp_2Zr(\eta^2$-pyridyl)(PMe_3) by X-ray crystallography.[2f]

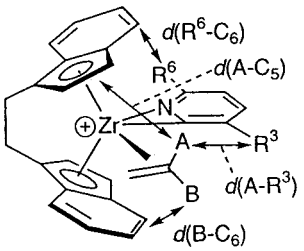

	R^6	R^3	A	B
12b	Ph	H	H	Me
12b'	Ph	H	Me	H
12c	H	H	H	Me
12c'	H	H	Me	H
12d	Me	Me	H	Me
12d'	Me	Me	Me	H

Figure 4. Key parameters used in structural comparisons of **12** and **12′**. Distances: d(A−R^3), H−H distances between A and R^3; d(A−C_5), H−H distances between A and the indenyl C_5 ring hydrogens; d(R^6−C_6), C−H distances between R^6 and the indenyl C_6 ring carbons; d(B−C_6), C−H distances between B and the indenyl C_6 carbons. Angles (not shown): tip angle (T), angle between the centroid−Zr−centroid and pyridyl C−N−C planes; slide angle (S), angle between the centroid−Zr−centroid and centroid−N−centroid planes.

To facilitate the structural analysis of **12**/**12′**, several key angles and distances were compared. These are defined and illustrated in Figure 4.

As shown in Table 3, **12b** was found to be 9.8 kcal/mol more stable than **12b′** and **12d** was found to be 8.4 kcal/mol more stable than **12d′**. Thus, for these cases, the more stable propene adduct is that which leads to the kinetic insertion product **6b** or **6d**. In contrast, no significant energy difference was found between **12c** and **12c′**, which implies that there is little diastereoselectivity in propene coordination to **5c** and is consistent with the low stereoselectivity observed in propene insertion of this species. We conclude that the kinetic stereoselectivities summarized in Table 2 reflect the relative stability of the diastereomeric adducts **12**/**12′**.[22]

Views of the optimized structures of **12b** and **12b′** and values for key structural parameters are given in Figure 5 and Table 3 and provide insight into the origin of the relative stability of these species. Complex **12b** exhibits a significant "tipping" ($T - 90 = 20.1°$) of the pyridyl ring out of the equatorial plane between the indenyl ligands, which results primarily from displacement of the pyridyl nitrogen out of the equatorial plane. The pyridyl tipping is caused by steric interactions between the pyridyl 6-substituent ($R^6 = Ph$) and the EBI C_6 ring. In the optimized structure, these groups are in close steric contact, as indicated by the phenyl-H/EBI-C

(19) (a) Piemontesi, F.; Camurati, I.; Resconi, L., Balboni, D. *Organometallics* **1995**, *14*, 1256. (b) Smith, J.; von Seyerl, J.; Huttner, G.; Brintzinger, H. H. *J. Organomet. Chem.* **1979**, *173*, 175.

(20) (a) Wu, Z.; Jordan, R. F.; Petersen, J. L. *J. Am. Chem. Soc.* **1995**, *117*, 5867. (b) Strömberg, S.; Christopher, J. C.; Lee, C. W.; Swenson, D. C.; Jordan, R. F., manuscript in preparation.

(21) For other d^0-metal olefin complexes see: (a) Kress, J.; Osborn, J. A. *Angew. Chem., Int. Ed. Engl.* **1992,** *31*, 1585. (b) Horton, A. D.; Orpen, A. G. *Organometallics* **1992**, *11*, 8. (c) Casey, C. P.; Hallenback, S. L.; Pollock, D. W.; Landis, C. R. *J. Am. Chem. Soc.* **1995**, *117*, 9770. For computational studies see: (d) Woo, T. K.; Fan, L.; Ziegler, T. *Organometallics* **1994**, *13*, 2252. (e) Lohrenz, J. C. W.; Woo, T. K.; Fan, L.; Ziegler, T. *J. Organomet. Chem.* **1995**, *497*, 91. (f) Yoshida, T.; Koga, N.; Morokuma, K. *Organometallics* **1995**, *14*, 746. (g) Kawamura-Kuribayashi, H.; Koga, N.; Morokuma, K. *J. Am. Chem. Soc.* **1992**, *114*, 2359. (h) Jensen, V. R.; Ystenes, M.; Wärnmark, K.; Åkermark, B.; Sevensson, M.; Siegbahn, P. E. M.; Bloomberg, M. R. A. *Organometallics* **1994**, *13*, 282.

(22) Steric interactions and trends in the relative energies of the insertion transition states linking propene adducts **12**/**12′** and metallacycle products **6**/**6′** are probably similar to those in **12**/**12′**.

Table 3. Energies and Key Structural Data for Optimized Structures of Model Propene Adducts 12, 12′, and Tipped-12′ from Molecular Modeling Calculations[a]

propene adduct	*E* (kcal/mol)	*T* (deg)	*S* (deg)	$d(A-R^3)$ (Å)	$d(A-C_5)$ (Å)	$d(R^6-C_6)$ (Å)	$d(B-C_6)$ (Å)
12b	367.2[b]	110.1	43.2	2.60	2.73	2.61	2.91
						3.02	3.09
12b′	377.4[b]	95.4	45.3	2.62	2.34	2.46	3.45
				2.69	2.66	2.75	
tipped-**12b′**	383.5[b]	110.1[d]	43.1	2.04	2.28	2.73	3.54
				2.87	2.77	2.97	
12c	348.3[c]	96.5	47.4	2.69	2.83	3.11	3.02
						3.42	
12c′	348.9[b]	92.3	47.4	2.69	2.32	3.13	3.11
					2.85	3.45	
12d	336.9[c]	105.4	44.6	2.44	2.86	2.88	3.01
						3.08	
12d′	345.3[b]	93.9	47.1	2.36	2.24	2.73	3.34
				2.39	2.81	3.01	
tipped-**12d′**	348.7[b]	105.4[e]	44.8	1.91	2.25	2.98	3.58
				2.55	2.57	3.36	

[a] Structural parameters are defined in Figure 4. [b] Indenyl-forward conformation. [c] Indenyl-back conformation. [d] *T* fixed at value found for **12b**. [e] *T* fixed at value found for **12d**.

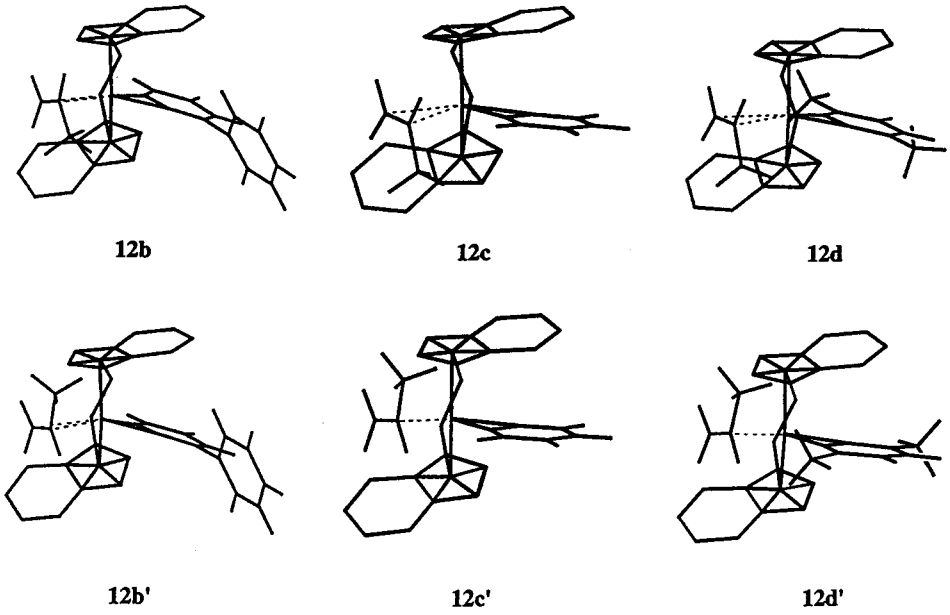

Figure 5. Optimized structures of **12b**/**12b′**, **12c**/**12c′**, and **12d**/**12d′** from molecular modeling. Hydrogen atoms have been omitted from the EBI ligand for clarity.

distances ($d(R^6-C6)$ = 2.6−3.0 Å).[23] In contrast, the pyridyl ring of **12b′** lies more nearly in the equatorial plane, which results in increased phenyl/EBI steric contact ($d(R^6-C6)$ = 2.5−2.8 Å) compared to that in **12b**. In this case pyridyl tipping is limited by propene/pyridyl steric contacts $d(A-R^3)$ = 2.6−2.7 Å). To probe the issue of pyridyl tipping further, we investigated the model complex "tipped-**12b′**", in which the tip angle *T* was fixed at the value observed for **12b**. As shown in Table 3, tipped-**12b′** is calculated to be 6.1 kcal/mol less stable than **12b′**. The pyridyl tipping in tipped-**12b′** decreases the phenyl/EBI steric interactions as expected but also dramatically increases the propene/pyridyl steric interactions ($d(A-R^3)$ < 2.2 Å). These results suggest that relief of pyridyl/EBI steric interactions in **12b′** by tipping of the pyridyl ring is limited by the propene/pyridyl steric interactions that this tipping would create.

Steric interactions in **12d**/**12d′** (Figure 5) are similar to those in **12b**/**12b′**. In **12d** steric contacts between the pyridyl 6-Me substituent (R^6) and the EBI C_6 ring are relieved by pyridyl tipping ($T - 90$ = 15.4°). However, for **12d′** pyridyl tipping is limited by steric interactions between the propene Me group and the pyridyl 3-Me group (R^3), which are in close contact ($d(A-R^3)$ = 2.36, 2.39 Å). Forced tipping of the pyridyl group in tipped-**12d′** (*T* fixed at the value found for **12d**) results in severe propene/pyridyl contact ($d(A-R^3)$ = 1.91 Å) and destabilization by 3.4 kcal/mol versus **12d′**. In contrast, no significant structural differences were found between **12c** and **12c′** (Figure 5). In this case, due to the absence of a substituent in the pyridyl 6-position, EBI/pyridyl steric interactions are not important and pyridyl tipping is not significant.

These computational results suggest that steric interactions between the η^2-pyridyl 6-substituent (R^6) and EBI C_6 ring strongly influence the relative stability of **12** and **12′**. In **12**, the EBI/pyridyl steric interactions are relieved by pyridyl tipping, whereas in **12′** pyridyl

(23) van der Waals radii of carbon (r_{vdW}(C)) and hydrogen (r_{vdW}(H)): for aliphatic C−H, r_{vdW}(C) = 1.7 Å and r_{vdW}(H) = 1.2 Å; for aromatic C−H, r_{vdW}(C) = 1.8 Å and r_{vdW}(H) = 1.0 Å. See: Bondi, A. *J. Phys. Chem.* **1964**, *68*, 441.

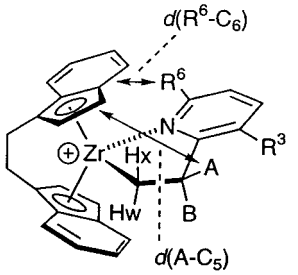

	R^6	R^3	A	B
6b	Ph	H	H	Me
6b'	Ph	H	Me	H
6c	H	H	H	Me
6c'	H	H	Me	H
6d	Me	Me	H	Me
6d'	Me	Me	Me	H

Figure 6. Labeling scheme and key structural parameters for **6**/**6′**. Distances: $d(R^6-C_6)$, C−H distances between R^6 and the indenyl C_6 ring carbons; $d(A-C_5)$, H−H distances between A and the indenyl C_5 ring hydrogens. Angles (not shown): tip angle (*T*), angle between the centroid−Zr−centroid and pyridyl C−N−C planes; slide angle (*S*), angle between the centroid−Zr−centroid and centroid−N−centroid planes.

tipping is limited by unfavorable propene/pyridyl steric contacts. The key requirement for stabilization of **12** versus **12′** is the presence of an η^2-pyridyl 6-substituent, which gives rise to strong EBI/pyridyl steric interactions. The preference for **12** is increased by the presence of an η^2-pyridyl 3-substituent (R^3), which enhances the pyridyl/propene steric interactions.

(ii) Comparison of *rac*-(EBI)Zr{η^2-(*C*,*N*)-CH_2CHMe(pyrid-2-yl)}$^+$ Species. To probe the factors which influence the stability of the propene insertion products, i.e. the thermodynamic **6**/**6′** product ratios, molecular modeling calculations were performed for **6b**/**6b′**, **6c**/**6c′**, and **6d**/**6d′**. Key structural parameters which are useful in comparing the structures of **6**/**6′** are defined in Figure 6.

The modeling procedure was first tested on [*S*,*S*,*S*-(EBI)Zr{η^2-(*C*,*N*)-CH_2CH(Bu)(6-methylpyrid-2-yl)}][BPh_4] (**7**; Scheme 3) which was structurally characterized by X-ray diffraction.[3,11] The Zr−N distance was constrained to be equal to the value determined crystallographically for **7**. Good agreement was found between the calculated structure and the X-ray structure.[24]

As summarized in Table 4, **6b** was found to be 16.8 kcal/mol more stable than **6b′**. This result is consistent with the fact that only **6b** is observed under conditions where **6b** and **6b′** should be at equilibrium (i.e., conditions where **6b** was shown to undergo reversible propene deinsertion). In contrast, no significant energy difference was found between **6c** and **6c′** or between **6d** and **6d′**. These results are consistent with the observed 50/50 thermodynamic ratios for these pairs of diastereomers.

The optimized structures of **6b** and **6b′** are shown in Figure 7. The pyridine group of **6b** is tipped out of the equatorial plane by 23° (*T* = 113°), and the metallacycle ring is puckered (Zr−C−C−py dihedral angle −37.1°). The β-Me group is in an equatorial position on the metallacycle ring and does not make close contact with the EBI ligand. The tipping of the pyridine ring in **6b** is more pronounced by ca. 10° than that observed in the crystallographically determined structures of [Cp_2Zr-{η^2(*C*,*N*)-CH_2CH_2(pyrid-2-yl)}][BPh_4] (**13**) and **7**, due to steric interactions between the R^6 = phenyl substituent and the EBI C_6 ring.[23,25] In contrast, the pyridine group in **6b′** is tipped to a lesser extent than in **6b**, which results in increased steric contact between the 6-phenyl group and the EBI C_6 ring; the $d(R^6-C_6)$ distances are ca. 0.2 Å shorter than in **6b**. In **6b′**, the metallacycle β-Me substituent is in an axial position and is forced into close contact with the EBI C_5 ring ($d(A-C_5)$ = 2.20 Å). Relief of this contact would require decreased pyridine tipping, which in turn would cause increased Ph/EBI interactions. **6b′** is destabilized relative to **6b** by the more severe R^6/EBI and Me/C_5 contacts.

The optimized structures of **6c** and **6c′** are very similar to each other (Figure 7). These species lack a pyridine 6-substituent, and therefore EBI/pyridyl steric interactions are less significant than in **6b**/**6b′**, as indicated by the larger values for the slide angle *S* and the $d(R^6-C_6)$ distances in **6c**/**6c′.** The optimized structures of **6d** and **6d′** are also very similar to each other (Figure 7). The tip angle *T* and the slide angle *S* are intermediate between the values calculated for **6b**/**6b′** and **6c**/**6c′**, as expected due to the intermediate size of the R^6 substituent (Me vs Ph or H). For both **6d** and **6d′** the metallacycle methyl and the pyridyl 3-Me groups are in close steric contact.[26] This steric crowding promotes the isomerization to the 2,1-insertion product **6d″**.

Conclusions

Chiral zirconocene η^2-pyridyl species of the type *rac*-(EBI)Zr(η^2-pyridyl)$^+$ (**5a**−**f**), which contain substituted η^2-pyridyl ligands, react readily with propene to yield the 1,2-insertion products [*rac*-(EBI)Zr{η^2(*C*,*N*)-CH_2-CHMe(pyridyl)}][$MeB(C_6F_5)_3$] (**6**/**6′**). Propene insertion of **5a**-**f** is under kinetic control at 23 °C and occurs with high diastereoselectivity in cases where the η^2-pyridyl ligand contains a 6-substituent ($R^6 \neq$ H; **6a**, de = 80%; **6b**, de > 96%; **6d**, de > 96%; **6e**, de = 80%). For these cases, the major diastereomer is that in which the metallacycle β-Me group points toward the EBI C_6 ring (configuration *S*,*S*,*S* (*R*,*R*,*R*), where the entries denote the configurations of the EBI bridgehead carbons and the metallacycle β-carbon, respectively). The diastereoselectivity is low in cases where R^6 = H (**6c′**, de = 20%; **6f**, de = 10%). Propene insertion of **5a**−**f** is reversible at 80 °C, and the kinetic **6**/**6′** mixtures evolve to the thermodynamic mixtures at this temperature. Molecular modeling studies of model *rac*-(EBI)Zr(η^2-pyridyl)(propene)$^+$ adducts suggest that steric interactions between the pyridyl R^6 substituent and the EBI C_6 ring cause a tipping of the pyridyl ligand, which influences the pyridyl/propene steric contacts and the facial selectivity of propene binding. The modeling results suggest that the more stable propene adduct diastereomer leads to the kinetic insertion product. The modeling results also suggest that pyridyl tipping influences the relative energies of the insertion products **6** and **6′** by affecting the steric contact between the axial β-substituent on the metallacycle and the indenyl C_5 ring. These results provide a basis for understanding

(24) Key structural parameters for **7** from X-ray structural analysis (and molecular modeling): tip angle *T* = 98.3° (modeled: 96.9°), slide angle *S* = 17.2° (modeled = 18.1°), $d(H_x-C_5)$ = 2.35, 3.12 Å (modeled: 2.43, 3.07 Å), $d(R^6-C_6)$ = 2.61, 3.06 Å (modeled: 2.76, 3.14 Å), Zr−C−C−py dihedral angle −35.6 (modeled: −39.7°).

(25) (a) Compound **13**: *T* = 99°, Zr−C−C−py dihedral angle −34.2°.[2b] (b) Compound **7**: *T* = 98.3°, Zr−C−C−py dihedral angle −39.7°.[3,11]

(26) Relevant H−H distances (Å) are as follows: **6d**, $d(A-R^3)$ = 2.26, $d(B-R^3)$ = 2.46; **6d′**, $d(A-R^3)$ = 2.20, 2.45, $d(B-R^3)$ = 2.30.

Table 4. Energies and Key Structural Data for Optimized Structures of Propene Insertion Products 6 and 6′[a]

insertion product	*E* (kcal/mol)	*T* (deg)	*S* (deg)	Zr−C−C−py dihedral angle (deg)	$d(R^6-C_6)$ (Å)	$d(A-C_5)$ (Å)
6b	169.8[b]	113.0	15.1	−37.1	2.56 2.59	2.27
6b′	186.0[b]	109.2	16.4	−18.1	2.38 2.39	2.20 2.90
6c	153.3[b]	97.8	27.7	−33.5	3.16 3.32	2.43
6c′	152.3[c]	93.7	27.4	−12.2	2.93 3.04	2.40
6d	141.6[c]	97.6	21.7	−5.5	2.67 2.84	3.38
6d′	142.5[c]	100.8	16.6	−17.6	2.61 2.77	2.43

[a] Structural parameters are defined in Figure 6. [b] Indenyl-back conformation. [c] Indenyl-forward conformation.

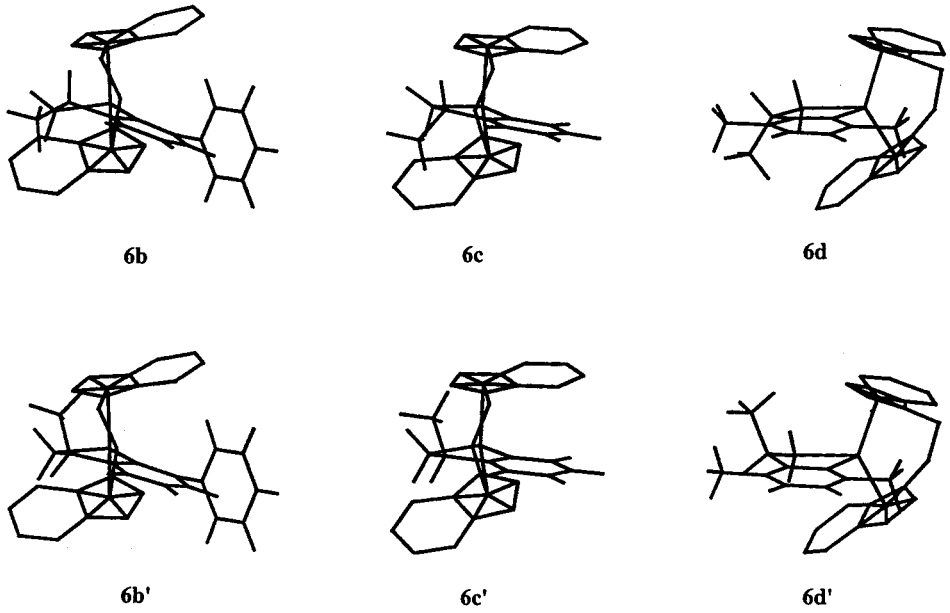

Figure 7. Optimized structures of **6b**/**6b′**, **6c**/**6c′**, and **6d**/**6d′** from molecular modeling. Hydrogen atoms have been omitted from the EBI ligand for clarity.

selectivity trends in stoichiometric and catalytic pyridine/olefin coupling reactions at chiral zirconocene centers and will be useful for guiding the selection of substrates for future studies.

Experimental Section

General Procedures. All experiments were carried out under N_2 using standard Schlenk techniques or a Vacuum Atmospheres glovebox. Hydrocarbon solvents were distilled from Na/benzophenone. Chlorinated solvents were distilled from CaH_2. Solvents were stored under N_2 prior to use. Pyridines were purchased from Aldrich and dried over molecular sieves (4 Å) for 2 days and distilled. Propene was purchased from Aldrich and used as received. *rac*-(EBI)$ZrMe_2$ was prepared by a literature procedure.[27] $B(C_6F_5)_3$ was obtained from Boulder Scientific.

NMR spectra were obtained on a Bruker AMX-360 spectrometer, in Teflon-valved or flame-sealed tubes, at ambient probe temperature (25 °C) unless otherwise indicated. ^1H and ^{13}C chemical shifts are reported versus Me_4Si and were determined by reference to the residual ^1H and ^{13}C solvent peaks. The ^1H and ^{13}C NMR data for noncoordinated anions are essentially identical for all compounds and are not listed.[28] COSY spectra were recorded in CD_2Cl_2 with a 5 s delay, TD(F_2) = 2048, TD(F_1) = 256, NS = 16, and SW = 11 ppm. NOESY spectra were recorded in CD_2Cl_2 with a 10 s delay, 1.4 s mixing time, TD(F_2) = 2048, TD(F_1) = 256, NS = 16, and SW = 11 ppm. Correlations were established by the presence of a cross-peak between two resonances. The presence of a NOESY correlation was interpreted as indicating distance between two correlating hydrogens of less than 4 Å. GC analyses were performed on a HP-5890 chromatograph with splitless injection equipped with a 15 m DB-1 column. EI-MS spectra were obtained with a VG-Analytical Trio-1 instrument (70 eV).

Generation of [*rac*-(EBI)ZrMe][$MeB(C_6F_5)_3$] (4). *rac*-(EBI)$ZrMe_2$ (15.1 mg, 0.0400 mmol), $B(C_6F_5)_3$ (20.5 mg, 0.0400 mmol), and CD_2Cl_2 (0.5 mL) were added to a resealable NMR tube and vigorously mixed, yielding an orange solution. The ^1H NMR spectrum was obtained after 10 min at 23 °C. ^1H NMR (CD_2Cl_2): δ 7.65 (d, J = 6.5 Hz, 1 H, indenyl C_6), 7.52−7.38 (m, 4 H, indenyl C_6), 7.27 (virtual triplet, J = 7.6 Hz, 1

(27) Diamond, G. M.; Petersen, J. L.; Jordan, R. F. *J. Am. Chem. Soc.* **1996**, *118*, 8024.

(28) Data for free $MeB(C_6F_5)_3^-$. ^1H NMR (CD_2Cl_2): δ 0.51 (br s, 3 H). $^{13}C\{^1H\}$ (CD_2Cl_2): δ 148.7 (d of m, J_{CF} = 237 Hz), 137.8 (d of m, J_{CF} = 242 Hz), 136.7 (d of m, J_{CF} = 242 Hz), 10.6 (m). Data for free $B(C_6F_5)_4^-$. $^{13}C\{^1H\}$ (CD_2Cl_2): δ 148.5 (d, J_{CF} = 238 Hz), 138.5 (d, J_{CF} = 243 Hz), 136.7 (d, J_{CF} = 243 Hz, 124.0 (br). Data for free BPh_4^-. ^1H NMR (CD_2Cl_2): δ 7.35 (m, 8 H), 7.04 (t, J = 7.4 Hz, 8 H), 6.90 (t, J = 7.2 Hz, 4 H). ^{13}C NMR (CD_2Cl_2): δ 163.5 (q, J_{BC} = 49 Hz), 135.4, 125.7, 121.7.

H, indenyl C_6), 7.05 (d, J = 3.1 Hz, 1 H, indenyl C_5), 6.69 (t, J = 7.6 Hz, 2 H, indenyl C_6), 6.38 (d, J = 3.2 Hz, 1 H, indenyl C_5), 6.15 (d, J = 2.9 Hz, 1 H, indenyl C_5), 6.03 (d, J = 2.9 Hz, 1 H, indenyl C_5), 3.81−3.72 (m, 1 H, CH_2CH_2), 3.58−3.54 (m, 2 H, CH_2CH_2), 3.46−3.39 (m, 1 H, CH_2CH_2), −0.38 (s, 3 H, $ZrCH_3$), −0.57 (br, 3 H, MeB).

Generation of *rac*-[(EBI)Zr{η^2(*C*,*N*)-pyrid-2-yl)}][MeB(C_6F_5)$_3$] (5a−f). *rac*-(EBI)$ZrMe_2$ (15.1 mg, 0.040 mmol), $B(C_6F_5)_3$ (20.5 mg, 0.040 mmol), and CD_2Cl_2 (0.5 mL) were added to a resealable NMR tube and vigorously mixed. In a drybox, the appropriate pyridine (0.0400 mmol) was added and the tube was shaken and then opened to release CH_4. After 20 min at 23 °C the reaction mixture was an orange solution and a ^{1}H NMR spectrum was recorded. **5a** was also analyzed by $^{13}C\{^1H\}$ NMR. NMR data for **5a**−**f** are listed below. The numbering system used for the η^2-pyridyl resonances is given in Scheme 1.

Data for 5a. ^{1}H NMR (CD_2Cl_2): δ 8.10 (d, J = 8.6 Hz, 1 H, pyridyl H3), 7.84 (d, J = 8.8 Hz, 1 H, pyridyl H5), 7.54 (virtual triplet, J = 7.4 Hz, 1 H, pyridyl H4), 7.37 (virtual triplet, J = 7.5 Hz, 1 H, indenyl C_6), 7.29 (m, 2 H, indenyl C_6), 7.10 (m, 2 H, indenyl C_6), 7.04 (d, J = 7.3 Hz, 1 H, indenyl C_6), 6.69 (virtual triplet, J = 7.5 Hz, 1 H, indenyl C_6), 6.49 (d, J = 8.5 Hz, 1 H, indenyl C_6), 6.48 (d, J = 3.0 Hz, 1 H, indenyl C_5), 6.39 (d, J = 3.0 Hz, 1 H, indenyl C_5), 6.03 (d, J = 3.0 Hz, 1 H, indenyl C_5), 5.32 (d, J = 3.0 Hz, 1 H, indenyl C_5), 3.90−3.60 (m, 4 H, CH_2CH_2), 2.27 (s, 3 H, pyridyl CH_3). $^{13}C\{^1H\}$ NMR (CD_2Cl_2): δ 201.2 (ipso, pyridyl ring), 156.1 (ipso, pyridyl ring), 140.3 (CH, pyridyl ring), 139.8 (CH, pyridyl ring), 127.7 (ipso), 127.6 (CH), 127.3 (CH), 126.7 (ipso), 126.6 (ipso), 126.4 (CH), 126.4 (CH), 124.3 (CH), 124.1 (ipso), 124.0 (CH), 123.5 (ipso), 123.4 (CH), 123.3 (ipso), 121.4 (CH), 114.7 (CH indenyl C_5), 110.6 (CH indenyl C_5), 101.3 (CH indenyl C_5), 100.7 (CH indenyl C_5), 30.9 (CH_2CH_2), 29.0 (CH_2CH_2), 22.3 (CH_3 pyridyl).

Data for 5b. ^{1}H NMR (CD_2Cl_2): δ 8.17 (d, J = 8.4 Hz, 1 H, pyridyl H3), 7.96−7.84 (m, 3 H), 7.76 (t, J = 8.4 Hz, 1 H, pyridyl H4), 7.60−7.21 (m, 7 H), 7.17 (d, J = 8.6 Hz, 1 H, indenyl C_6), 6.96 (d, J = 8.5 Hz, 1 H, indenyl C_6), 6.77 (virtual triplet, J = 7.6 Hz, 1 H, indenyl C_6), 6.56 (virtual triplet, J = 7.5 Hz, 1 H, indenyl C_6), 6.50 (d, J = 3.0 Hz, 1 H, indenyl C_5), 6.45 (d, J = 3.0 Hz, 1 H, indenyl C_5), 6.18 (d, J = 3.0 Hz, 1 H, indenyl C_5), 5.32 (d, J = 3.0 Hz, 1 H, indenyl C_5), 3.90−3.61 (m, 4 H, CH_2CH_2).

Data for 5c. ^{1}H NMR (CD_2Cl_2): δ 8.41 (d, J = 8.3 Hz, 1 H, pyridyl H6), 8.17 (d, J = 8.5 Hz, 1 H, pyridyl), 7.78 (t, J = 7.5 Hz, 1 H, pyridyl), 7.47 (t, J = 7.5, 1 H, pyridyl), 7.42 (d, J = 8.8 Hz, 1 H, indenyl C_6), 7.37−7.32 (m, 3 H), 6.87 (virtual triplet, J = 7.7 Hz, 1 H, indenyl C_6), 6.78−6.51 (m, 3H), 6.50 (d, J = 2.9 Hz, 1 H, indenyl C_5), 6.18 (d, J = 2.9 Hz, 1 H, indenyl C_5), 5.91 (d, J = 3.0 Hz, 1 H, indenyl C_5), 5.41 (d, J = 3.0 Hz, 1 H, indenyl C_5), 3.81−3.53 (m, 4 H, CH_2CH_2).

Data for 5d. ^{1}H NMR (CD_2Cl_2): δ 7.81 (d, J = 7.6 Hz, 1 H, pyridyl), 7.52−7.33 (m, 3 H), 7.23 (virtual triplet, J = 8.5 Hz, 1 H, indenyl C_6), 7.17−7.05 (m, 2 H), 6.96 (d, J = 8.6 Hz, 1 H, indenyl C_6), 6.71 (d, J = 3.0 Hz, 1 H, indenyl C_5), 6.48 (d, J = 3.0 Hz, 1 H, indenyl C_5), 6.29 (d, J = 8.6 Hz, 1 H, indenyl C_6), 6.17 (d, J = 3.0 Hz, 1 H, indenyl C_5), 5.57 (d, J = 3.0 Hz, 1 H, indenyl C_5), 3.89−3.52 (m, 4 H, CH_2CH_2), 2.29 (s, 3 H, CH_3 pyridyl), 2.23 (s, 2 H, CH_3 pyridyl).

Data for 5e. ^{1}H NMR (CD_2Cl_2): δ 8.05 (d, J = 8.6 Hz, 1 H, pyridyl H3), 7.89 (d, J = 8.7 Hz, 1 H, pyridyl H4), 7.66 (d, J = 8.5 Hz, 1 H, indenyl C_6), 7.40−7.22 (m, 3 H), 6.91 (d, J = 8.7 Hz, 1 H, indenyl C_6), 6.73 (virtual triplet, J = 7.7 Hz, 1 H, indenyl C_6), 6.66−6.50 (m, 2H), 6.52 (d, J = 3.0 Hz, 1 H, indenyl C_5), 6.48−6.37 (m, 2 H), 6.07 (d, J = 3.0 Hz, 1 H, indenyl C_5), 5.87 (d, J = 3.0 Hz, 1 H, indenyl C_5), 5.52 (d, J = 3.0 Hz, 1 H, indenyl C_5), 3.83−3.53 (m, 4 H, CH_2CH_2).

Data for 5f. ^{1}H NMR (CD_2Cl_2): δ 8.37 (s, 1 H, pyridyl H6), 7.85 (s, 1 H, pyridyl H4), 7.58 (d, J = 8.6 Hz, 1 H, indenyl C_6), 7.41 (d, J = 8.6 Hz, 1 H, indenyl C_6), 7.33 (virtual triplet, J = 7.6 Hz, 1H, indenyl C_6), 7.10 (virtual triplet, J = 7.7 Hz, indenyl C_6), 7.06 (d, J = 2.9 Hz, 1 H, indenyl C_5), 6.95 (d, J = 8.7 Hz, 1 H, indenyl C_6), 6.61 (d, J = 2.9 Hz, 1 H, indenyl C_5), 6.43−6.37 (m, 3H), 6.22 (d, J = 2.9 Hz, 1 H, indenyl C_5), 6.02 (d, J = 2.9 Hz, 1 H, indenyl C_5), 3.91−3.54 (m, 4 H, CH_2CH_2), 2.27 (s, 3 H, CH_3 pyridyl), 2.23 (s, 3 H, CH_3 pyridyl).

[*rac*-(EBI)Zr(η^2-6-methylpyrid-2-yl)(2-methylpyridine)][BPh_4]. *rac*-(EBI)$ZrMe_2$ (386 mg, 1.00 mmol) and 2-methylpyridine (296 μL, 3.00 mmol) were added to a mixture of hexane and diethyl ether (20 mL, 1/1 mixture by volume). The resulting suspension was vigorously stirred at 23 °C, and [$HNBu_3$][BPh_4] (496 mg, 1.00 mmol) was added. The reaction vessel was vented to release methane. The suspension was stirred at 23 °C overnight, and the color turned from light yellow to pink. The solid was isolated by filtration, washed with hexane (2 × 3 mL), and dried under vacuum. Yield: 0.78 g (91%). Anal. Calcd for $C_{56}H_{49}BN_2Zr$: C, 78.94; H, 5.80; N, 3.29. Found: C, 78.93; H, 5.73; N, 3.17. The NMR spectra established the presence of two isomers in a 3/2 ratio (N-outside and N-inside). **Major isomer:** ^{1}H NMR (CD_2Cl_2) δ 7.73 (m, 3 H), 7.56 (m, 2 H), 7.35−6.78 (m, 4 H), 7.51 (d, J = 7.4 Hz, 1 H), 6.48−6.14 (m, 7 H), 5.70 (d, J = 2.5 Hz, 1 H, indenyl C_5), 5.03 (d, J = 2.7 Hz, 1 H, indenyl C_5), 4.15−3.45 (m, 4 H), 1.84 (s, 3 H); $^{13}C\{^1H\}$ NMR (CD_2Cl_2) δ 197.9, 159.6, 150.1, 149.0, 140.0, 139.3, 131.3, 130.7, 128.0, 127.2, 126.5, 126.3, 125.4, 125.0, 124.3, 124.1, 123.7, 123.0, 122.9, 120.8, 118.6, 117.7, 116.1, 113.9, 97.7, 94.2, 32.0, 29.1, 24.2, 21.2. **Minor isomer:** ^{1}H NMR (CD_2Cl_2) δ 8.23 (t, J = 7.5 Hz, 1 H), 8.22 (d, J = 8.2 Hz, 1 H), 7.49 (d, J = 5.3 Hz, 1 H), 6.81 (dd, 1 H), 6.39 (d, J = 2.5 Hz, 1 H, indenyl C_5), 6.06 (d, J = 2.4 Hz, 1 H, indenyl C_5), 4.70 (d, J = 3.1 Hz, 1 H, indenyl C_5), 4.13−3.45 (m, 4 H), 2.07 (s, 3 H), 1.90 (s, 3 H); $^{13}C\{^1H\}$ NMR (CD_2Cl_2) δ 199.2, 160.6, 151.2, 149.2, 139.4, 131.6, 129.6, 128.6, 126.9, 125.5, 124.9, 124.6, 123.2, 122.3, 121.3, 121.2, 121.1, 119.5, 113.4, 94.9, 93.2, 32.2, 28.8, 25.8, 21.5.[29]

[*rac*-(EBI)Zr(η^2-6-phenylpyrid-2-yl)(2-phenylpyridine)][B(C_6F_5)$_4$]. *rac*-(EBI)$ZrMe_2$ (386 mg, 1.00 mmol) and 2-phenylpyridine (296 μL, 3.00 mmol) were added to a mixture of hexane and diethyl ether (20 mL, 1/1 mixture by volume). The resulting suspension was vigorously stirred at 23 °C, and [$HNMe_2Ph$][$B(C_6F_5)_4$] (796 mg, 1.00 mmol) was added. The reaction vessel was vented to release CH_4. The suspension was stirred overnight, and the color turned from light yellow to pink. The solid was isolated by filtration, washed with hexane (2 × 3 mL), and dried under vacuum. Yield: 0.81 g (92%). Anal. Calcd for $C_{66}H_{33}BF_{20}N_2Zr$: C, 59.32; H, 2.48; N, 2.02. Found: C, 57.95; H, 2.49; N, 2.09. The NMR spectra established that this species exists as a single isomer, presumably the N-outside isomer. ^{1}H NMR (CD_2Cl_2): δ 8.32 (d, J = 8.6 Hz, 1 H), 7.75−7.00 (m, 21 H), 6.54 (d, J = 8.6 Hz, 1 H), 6.43 (dd, J = 5.8, 5.3 Hz, 1 H), 6.36 (d, J = 8.7 Hz, 1 H), 6.21 (dd, J = 5.8, 5.5 Hz, 1 H), 5.35 (d, J = 3.0 Hz, 1 H, indenyl C_5), 5.16 (d, J = 2.9 Hz, 1 H, indenyl C_5), 4.96 (d, J = 2.9 Hz, 1 H, indenyl C_5), 3.90−3.81 (m, 2 H), 3.60−3.44 (m, 2 H). $^{13}C\{^1H\}$ NMR (CD_2Cl_2): δ 201.8, 162.3, 151.3, 150.5, 139.9, 139.8, 139.3, 136.2, 132.3, 130.8, 129.7, 129.4, 129.3, 129.2, 129.1, 127.8, 127.5, 126.7, 126.2, 125.8, 125.5, 125.1, 125.0, 124.9, 124.4, 124.3, 123.8, 122.2, 121.8, 121.6, 120.9, 119.8, 113.5, 98.4, 94.4, 32.2, 29.8.

Generation of *rac*-[(EBI)Zr{η^2(*C*,*N*)-CH_2CHMe-(pyridyl)}][MeB(C_6F_5)$_3$] (6a/6a′, 6b, 6c/6c′, 6d, 6e/6e′, 6f/6f′). *rac*-(EBI)$ZrMe_2$ (15.1 mg, 0.0400 mmol), $B(C_6F_5)_3$ (20.5 mg, 0.0400 mmol), and CD_2Cl_2 (0.5 mL) were added to a resealable NMR tube and vigorously mixed. In a drybox, the appropriate pyridine (0.040 mmol) was added, and the tube was shaken and then opened to release CH_4. Outside the drybox, the tube was attached to a vacuum line *via* a gas bulb. The tube was cooled to −196 °C (liquid N_2) and evacuated, and propene (286 Torr in 25.8 mL, 0.400 mmol, 10.0 equiv) measured *via* the gas bulb was condensed into the tube. The

(29) ^{1}H NMR resonances in the range δ 7.8−6.4 could not be assigned due to overlap of the signals for the major and minor isomers and BPh_4^-.

tube was warmed to 23 °C, and the reaction was periodically monitored by ^{1}H NMR. When the reaction was complete, the volatiles were removed under high vacuum overnight. CD_2Cl_2 (0.5 mL) was added to the tube by vacuum transfer, and the 1D and 2D NMR spectra were recorded.

NMR assignments are listed based on the basis of the numbering scheme in Figure 2. For clarity, the pyridyl−Me carbons are denoted by the pyridyl carbon they are connected to. For example, for **6d**, the two methyl groups on the pyridyl ring are denoted by CH_3 on C3″ and CH_3 on C6″. For the 2D NMR correlations, the hydrogens in parentheses in normal text are the ones corresponding to the chemical shifts listed before the parentheses and the hydrogens in italics are the correlated atoms.

Data for 6a. ^{1}H NMR (CD_2Cl_2): δ 7.77 (d, J = 8.7 Hz, 1 H, H_f), 7.63 (t, J = 7.8 Hz, 1 H, H_r), 7.49 (dd, J = 8.4, 7.6, 1 H, H_n), 7.41 (d, J = 8.6 Hz, 1 H, H_p), 7.30 (d, J = 8.6 Hz, 1 H, H_m), 7.26 (dd, J = 7.6, 6.7 Hz, 1 H, H_o), 7.18 (d, J = 3.3 Hz, 1 H, H_b), 7.12 (d, J = 7.6 Hz, 1 H, H_q), 7.12 (dd, obscured, 1 H, H_e), 7.00 (d, J = 8.7 Hz, 1 H, H_c), 6.86 (d, J = 7.6 Hz, 1 H, H_s), 6.65 (dd, J = 7.5, 6.7 Hz, 1 H, H_d), 6.57 (d, J = 3.1 Hz, 1 H, H_k), 6.25 (d, J = 3.0 Hz, 1 H, H_l), 5.96 (d, J = 3.4 Hz, 1 H, H_a), 3.93 (m, 1 H, H_g), 3.63 (m, 1 H, H_h), 3.59 (m, 1 H, H_i), 3.49 (virtual septet, J = 6.8 Hz, 1 H), 3.48 (m, 1 H, H_j), 1.15 (s, 3 H, H_t), 1.14 (d, J = 6.6 Hz, 3 H, H_v), 0.32 (dd, J = 13.1, 5.3 Hz, 1 H, H_x), −0.08 (dd, J = 12.9, 11.8 Hz, 1 H, H_w). ^{13}C{^{1}H} NMR (CD_2Cl_2): δ 170.6 (ipso), 155.7 (ipso), 142.6 (C4″), 130.7 (ipso), 128.5 (C5′), 127.8 (C6′), 127.7 (C6), 126.9 (ipso), 126.6, 126.1 (C5), 125.9 (C4′), 125.6 (ipso), 125.2 (ipso), 125.1 (C5″), 124.7 (ipso), 124.0 (C7′), 123.7 (C4), 122.8 (ipso), 121.5 (C7, C3″), 116.9 (C2), 116.1 (C2′), 109.0 (C3), 103.9 (C3′), 66.9 (C9″), 40.5 (C8″), 29.3 (C10), 28.7 (C10′), 25.6 (C10″), 23.4 (CH_3 on C6″). Key ^{1}H−^{1}H COSY correlations: δ 7.77 (H_f, H_e), 7.63 (H_r, H_s, H_q), 7.49 (H_n, H_o, H_m), 7.41 (H_p, H_o), 7.30 (H_m, H_n), 7.26 (H_o, H_n, H_p), 7.18 (H_b, H_a), 7.12 (H_q, H_r), 7.12 (H_e, H_f, H_d), 7.00 (H_c, H_d), 6.86 (H_s, H_r), 6.65 (H_d, H_e, H_c), 6.57 (H_k, H_l), 6.25 (H_l, H_k), 5.96 (H_a, H_b), 3.93 (H_g, H_h, H_i, H_j), 3.63 (H_j, H_g, H_i, H_h), 3.59 (H_i, H_g, H_h, H_j), 3.49 (H_u, H_v, H_x, H_w), 3.48 (H_h, H_g, H_j, H_i), 1.14 (H_v, H_u), 0.32 (H_x, H_u, H_w), −0.08 (H_w, H_u, H_x). Key ^{1}H−^{1}H NOESY correlations: δ 7.77 (H_f, H_g, H_t, H_k), 7.49 (H_n, H_w), 7.41 (H_p, H_a, H_j), 7.30 (H_m, H_l, H_w), 7.18 (H_b, H_c, H_x, H_u, H_w), 7.12 (H_q, H_v), 7.12, 7.00 (H_c, H_b, H_u), 6.86 (H_s, H_t), 6.65 (H_d, H_k, H_t), 6.57 (H_k, H_d, H_f, H_t, H_g, H_i), 6.25 (H_l, H_m, H_t), 5.96 (H_a, H_p, H_x, H_h), 3.93 (H_g, H_f, H_k), 3.63 (H_j, H_a), 3.59 (H_i, H_k), 3.49 (H_u, H_b, H_c), 3.48 (H_h, H_p), 1.15 (H_t, H_s, H_k, H_l, H_f, H_d), 1.14 (H_v, H_w, H_x, H_q), 0.32 (H_x, H_v, H_b, H_a), −0.08 (H_w, H_v, H_m, H_n, H_b).

Data for 6a′. ^{1}H NMR (CD_2Cl_2): δ 7.96 (d, J = 8.8 Hz, 1 H, H_f), 7.67 (t, J = 7.8 Hz, 1 H, H_r), 7.51 (d, J = 6.8 Hz, 1 H), 6.95 (d, J = 3.1 Hz, 1 H, H_b), 6.93 (dd, J = 6.9, 1 H), 6.85 (partially obscured, 1 H, H_s), 6.46 (d, J = 3.2 Hz, 1 H, H_k), 6.27 (d, J = 3.2 Hz, 1 H, H_l), 5.96 (d, J = 3.4 Hz, 1 H, H_a), 2.78 (sextet, J = 7.4 Hz, 1 H, H_u), 2.51 (dd, J = 13.1, 8.9, 1 H, H_x), 1.22 (d, J = 6.8 Hz, 3 H, H_v), 0.82 (s, 3 H, H_t), −1.79 (dd, J = 13.1, 7.9, 1 H, H_w). ^{13}C{^{1}H} NMR (CD_2Cl_2): δ 127.9 (CH), 127.7 (CH), 119.8 (CH), 118.7 (CH), 109.9 (CH), 104.4 (CH), 67.8 (C9″), 44.2 (C8″), 30.5 (C10), 29.6 (C10′), 24.7 (C7″), 23.8 (CH_3 on C6″). Key ^{1}H−^{1}H COSY correlations: δ 6.95 (H_b, H_a), 6.46 (H_l, H_k), 6.27 (H_k, H_l), 5.96 (H_a, H_b), 2.78 (H_u, H_v), 2.51 (H_x, H_w), 1.22 (H_v, H_u), −1.79 (H_w, H_x). Key ^{1}H−^{1}H NOESY correlations: δ (H_f, H_k, H_l), 6.95 (H_b, H_x), 6.85 (H_s, H_t), 6.46 (H_l, H_f, H_t), 6.27 (H_k, H_t, H_k), 5.96 (H_a, H_x), 2.78 (H_u, H_w), 2.51 (H_x, H_b, H_a, H_v), 1.22 (H_v, H_x), 0.82 (H_t, H_l, H_k, H_s), −1.79 (H_w, H_u).

Data for 6b. ^{1}H NMR (CD_2Cl_2): δ 8.24 (d, J = 8.7 Hz, 1 H, H_f), 7.96 (t, J = 7.9 Hz, 1 H, H_r), 7.74 (t, J = 8.7 Hz, 1 H, Ph ring), 7.55 (dd, J = 8.6, 6.0 Hz, 1 H, H_e), 7.48 (t, J = 8.0 Hz, 2 H, Ph ring), 7.47 (d, J = 8.0 Hz, 1 H, H_c), 7.45 (d, J = 7.7 Hz, 1 H, H_s), 7.35 (d, J = 8.0 Hz, 1 H, H_q), 7.32−7.26 (m, 3 H, H_o, H_d, H_p), 7.10 (dd, J = 8.6, 6.0 Hz, 1 H, H_n), 7.01 (d, J = 3.2 Hz, 1 H, H_b), 6.63 (d, J = 8.6 Hz, 1 H), 6.27 (d, J = 3.3 Hz, 1 H, H_a), 5.95 (br s, 2 H, Ph ring), 5.77 (d, J = 3.2 Hz, 1 H, H_k), 3.67 (m, 2 H, H_u, H_g), 3.57 (d, J = 3.1 Hz, 1 H, H_l), 3.55 (m, 1 H, H_i), 3.36 (m, 2 H, H_h, H_j), 1.19 (d, J = 6.5 Hz, 3 H, H_v), 0.65 (dd, J = 12.6, 3.7 Hz, 1 H, H_x), −1.13 (virtual triplet, J = 12.4 Hz, 1 H, H_w). ^{13}C{^{1}H} NMR (CD_2Cl_2): δ 158.8 (ipso), 142.5 (C4″), 140.5 (ipso), 135.3 (CH Ph ring), 133.0 (CH Ph ring), 128.0 (C5′), 127.9 (ipso), 127.9, 127.7 (ipso), 127.5 (ipso), 126.9 (ipso), 126.6 (C6), 125.3 (ipso), 125.1, 124.7, 124.3 (ipso), 123.9 (C4), 123.8 (ipso), 123.7 (C4′), 122.7 (C5″), 122.0 (C8″), 121.9 (C3″), 120.0 (C2), 111.7 (C2′), 104.2 (C3), 103.3 (C3′), 72.2 (C7″), 42.0 (C8″), 29.9 (C10), 28.2 (C10′), 23.6 (C9″). Key ^{1}H−^{1}H COSY correlations: δ 8.24 (H_f, H_e), 7.96 (H_r, H_q, H_s), 7.55 (H_e, H_d, H_f), 7.47 (H_c, H_d), 7.45 (H_s, H_r), 7.35 (H_q, H_r), 7.32−7.26 (H_d, H_o, H_p, H_e, H_c, H_n), 7.10 (H_n, H_m), 7.01 (H_b, H_a), 6.63 (H_m, H_n), 6.27 (H_a, H_b), 5.95 (H_t, H_u), 5.77 (H_k, H_l), 3.67 (H_u, H_g, H_x, H_w, H_{g-j}), 3.57 (H_l, H_k), 3.55 (H_i, H_{g-h}, H_j), 3.36 (H_h, H_j, H_g, H_i), 1.19 (H_v, H_u), 0.65 (H_x, H_u, H_w), −1.13 (H_w, H_u, H_x). Key ^{1}H−^{1}H NOESY correlations: δ 8.24 (H_f, H_k, H_g), 7.47 (H_c, H_b, H_t), 7.45 (H_s, H_t), 7.35 (H_q, H_v), 7.32−7.26 (H_d, H_o, H_p, H_j), 7.10−7.01 (H_b, H_c, H_x, H_u), 6.63 (H_m, H_w, H_l), 6.27 (H_a, H_h, H_x), 5.95 (H_t, H_s, H_c), 5.77 (H_k, H_f), 3.67 (H_u, H_g, H_b, H_f), 3.57 (H_l, H_m, H_u), 3.55 (H_i, H_f, H_p), 3.36 (H_h, H_j, H_p, H_a), 1.19 (H_v, H_q), 0.65 (H_x, H_b, H_a), −1.13 (H_w, H_m, H_a).

Data for 6c. ^{1}H NMR (CD_2Cl_2): δ 7.80 (dd, J = 8.1, 7.6 Hz, 1 H, H_r), 7.66 (d, J = 8.7 Hz, 1 H, H_f), 7.45 (m, 2 H, H_n, H_o), 7.40 (d, J = 3.8 Hz, 1 H, H_b), 7.36 (d, J = 8.6 Hz, 1 H, H_p), 7.30 (d, J = 8.2 Hz, 1 H, H_q), 7.23 (obscured, 1 H, H_o), 7.13 (dd, J = 6.5, 5.6 Hz, H_s), 7.07 (dd, J = 8.6, 6.7 Hz, 1 H, H_e), 7.01 (d, J = 8.6 Hz, 1 H, H_c), 6.84 (d, J = 3.5 Hz, 1 H, H_k), 6.53 (d, J = 6.3 Hz, 1 H, H_t), 6.41 (dd, J = 8.6, 7.6 Hz, 1 H, H_d), 6.18 (d, J = 3.5 Hz, 1 H, H_l), 6.03 (d, J = 3.4 Hz, 1 H, H_a), 4.12 (m, 1 H, H_g), 3.70 (m, 2 H, H_i, H_j), 3.54 (m, 1 H, H_h), 3.52 (m, 1 H, H_u), 1.15 (d, J = 6.7 Hz, 3 H, H_v), 0.59 (dd, J = 13.1, 5.6, 1 H, H_x), −0.17 (dd, J = 12.9, 11.6 Hz, 1 H, H_w). ^{13}C{^{1}H} NMR (CD_2Cl_2): δ 146.1 (C6″), 142.2 (C4″), 128.3 (C6′), 128.1 (C6), 127.4 (C5′), 126.6 (C4′), 125.8 (C5), 124.2 (C4), 124.1 (C3″), 123.3 (C5″), 122.5 (C7′), 119.7 (C7), 116.9 (C2), 116.3 (C2′), 109.3 (C3′), 109.2 (C3), 63.9 (C7″), 41.7 (C8″), 29.1 (C10′), 28.4 (C10), 23.3 (C8″). Key ^{1}H−^{1}H COSY correlations: δ 7.80 (H_r, H_s, H_q), 7.66 (H_f, H_e), 7.45 (H_n, H_m, H_o), 7.40 (H_b, H_a), 7.36 (H_p, H_o), 7.30 (H_q, H_r), 7.23 (H_o, H_p, H_n), 7.13 (H_s, H_r, H_t), 7.07 (H_e, H_f, H_d), 7.01 (H_c, H_d), 6.84 (H_k, H_l), 6.53 (H_t, H_s), 6.41 (H_d, H_e, H_c), 6.18 (H_l, H_k), 6.03 (H_a, H_b), 4.12 (H_g, H_h), 3.54 (H_h, H_g), 3.52 (H_u, H_x, H_w, H_v), 1.15 (H_v, H_u), 0.59 (H_x, H_w, H_u), −0.17 (H_w, H_x, H_u). Key ^{1}H−^{1}H NOESY correlations: δ 7.66 (H_f, H_g), 7.45 (H_n, H_m, H_w), 7.40 (H_b, H_w, H_x, H_u), 7.36 (H_p, H_a, H_w), 7.30 (H_q, H_v), 7.23 (H_o, H_w), 7.01 (H_c, H_w, H_u, H_t), 6.84 (H_k, H_i, H_g), 6.53 (H_t, H_k, H_l, H_c), 6.18 (H_l, H_w, H_t), 6.03 (H_a, H_x, H_h, H_j, H_p), 4.12 (H_g, H_f, H_k), 3.70 (H_j, H_i, H_k, H_a), 3.54 (H_h, H_a), 3.52 (H_u, H_b, H_c), 1.15 (H_v, H_q), 0.59 (H_x, H_a, H_b), −0.17 (H_w, H_n, H_m, H_b, H_o).

Data for 6c′. ^{1}H NMR (CD_2Cl_2): δ 7.79 (dd, J = 7.7, 6.1 Hz, 1 H, H_r), 7.72 (d, J = 8.7 Hz, 1 H, H_f), 7.60 (d, J = 8.6 Hz, 1 H, H_m), 7.45 (obscured, 3 H, H_n, H_o, H_p), 7.30 (dd, J = 7.6, 6.6 Hz, 1 H, H_b), 7.23 (d, J = 3.0, 1 H, H_b), 7.21 (obscured, 1 H, H_q), 7.17 (d, J = 8.6 Hz, 1 H, H_c), 7.10 (dd, J = 7.5, 5.5 Hz, 1 H, H_s), 6.72 (dd, J = 8.6, 6.7 Hz, 1 H, H_d), 6.49 (d, J = 3.4 Hz, 1 H, H_k), 6.25 (d, J = 3.4 Hz, H_l), 6.24 (d, J = 3.8 Hz, 1 H, H_a), 6.15 (d, J = 5.6 Hz, 1 H, H_t), 4.02 (m, 1 H, H_g), 3.76 (m, 1 H, H_j), 3.66 (m, 1 H, H_i), 3.61 (m, 1 H, H_h), 3.16 (virtual sextet, J = 7.3 Hz, 1 H, H_u), 2.58 (dd, J = 13.5, 8.9 Hz, 1 H, H_x), 1.23 (d, J = 6.8 Hz, 3 H, H_v), −1.75 (dd, J = 13.5, 7.2 Hz, 1 H, H_w). ^{13}C{^{1}H} NMR (CD_2Cl_2): δ 144.8 (C6″), 142.3 (C4″), 128.8 (C6), 127.8 (C6′), 126.8 (C5′), 126.5 (C5), 126.1 (C4′), 124.9 (C4), 124.0 (C3″), 123.7 (C5″), 122.1 (C7′), 120.9 (C7), 118.5 (C2), 116.5 (C2′), 111.4 (C3), 108.6 (C3′), 64.5 (C7″), 44.9 (C8″), 29.2 (C10), 28.4 (C10′), 24.0 (C9″). Key ^{1}H−^{1}H COSY: δ 7.79 (H_r, H_s, H_q), 7.72 (H_f, H_e), 7.60 (H_m, H_n), 7.45 (H_{n-p}, H_m), 7.30 (H_e, H_f, H_d), 7.23 (H_b, H_a), 7.21 (H_q, H_r), 7.17 (H_c, H_d), 7.10 (H_s, H_t, H_r), 6.72 (H_d, H_c, H_e), 6.49 (H_k, H_l), 6.25 (H_l, H_k), 6.24 (H_a, H_b), 6.15 (H_t, H_s), 4.02 (H_g, H_h, H_j, H_i), 3.76 (H_j, H_i, H_g), 3.66 (H_i, H_j, H_g), 3.61 (H_h, H_g), 3.16 (H_u, H_v, H_w, H_x), 2.58 (H_x, H_w, H_u), 1.23 (H_v, H_u), −1.75 (H_w, H_x, H_u). Key ^{1}H−^{1}H

NOESY: δ 7.72 (H_f, H_g, H_k), 7.60 (H_m, H_x, H_u, H_l), 7.45 (H_{n-p}, H_j, H_w, H_a), 7.30 (H_e, H_t), 7.23 (H_b, H_x, H_v), 7.21 (H_q, H_v), 7.17 (H_c, H_v), 6.49 (H_k, H_g, H_i, H_f), 6.25 (H_l, H_m), 6.24 (H_a, H_h, H_j, H_p), 6.15 (H_t, H_e), 4.02 (H_g, H_k), 3.76 (H_j, H_p), 3.66 (H_i, H_k), 3.16 (H_u, H_m, H_b), 2.58 (H_x, H_m, H_b), 1.23 (H_v, H_b, H_q, H_c), −1.75 (H_w, H_n, H_o, H_p).

Data for 6d. ^{1}H NMR (CD_2Cl_2): δ 7.95 (d, J = 8.3 Hz, 1 H, H_f), 7.62−7.59 (m, 2 H, H_m, H_n), 7.57 (d, J = 7.8 Hz, 1 H, H_r), 7.51 (d, J = 8.6 Hz, 1 H, H_p), 7.31 (dd, J = 8.6, 5.9 Hz, 1 H, H_o), 7.20 (dd, J = 8.3, 6.6 Hz, H_e), 6.87 (d, J = 7.8 Hz, 1 H, H_s), 6.82 (d, J = 3.1 Hz, 1 H, H_b), 6.76 (dd, J = 7.6, 6.6 Hz, 1 H, H_d), 6.59 (d, J = 3.1 Hz, 1 H, H_k), 6.52−6.48 (m, 2 H, H_c, H_l), 5.92 (d, J = 3.2 Hz, 1 H, H_a), 3.85−3.65 (m, 2 H, H_g, H_i), 3.66−3.51 (m, 3 H, H_h, H_j, H_u), 2.37 (s, 3 H, H_q), 1.55 (dd, J = 13.8, 4.6 Hz, 1 H, H_x), 0.99 (s, 3 H, H_t), 0.86 (d, J = 6.9 Hz, 3 H, H_v), −1.21 (dd, J = 13.8, 9.6 Hz, 1 H, H_w). ^{13}C{^{1}H} NMR (CD_2Cl_2): δ 161.1 (C2″), 152.5 (C6″), 145.2 (C4″), 131.9 (C9), 131.3 (C9′), 128.1 (C5′, C6′), 127.7 (C7), 127.2 (C3″), 127.1 (C6), 126.7 (C4′), 125.6 (C8), 125.2 (C8′), 125.1 (C5″), 124.3 (C7′), 123.4 (C1), 122.9 (C1′), 122.7 (C4), 122.0 (C7), 120.1 (C2), 118.1 (C2′), 106.5 (C3), 102.6 (C3′), 64.4 (C7″), 40.2 (C8″), 30.2 (C10), 29.7 (C10′), 25.1 (C9″), 23.8 (CH_3 pyridyl on C6″), 18.7 (CH_3 pyridyl on C3″). Key ^{1}H−^{1}H COSY correlations: δ 7.95 (H_f, H_e), 7.62−7.59 (H_n, H_m, H_o), 7.57 (H_r, H_s), 7.51 (H_p, H_o), 7.31 (H_o, H_p, H_n), 7.20 (H_e, H_d, H_f), 6.87 (H_s, H_r), 6.82 (H_b, H_a), 6.76 (H_d, H_e, H_c), 6.59 (H_k, H_l), 6.52−6.48 (H_c, H_l, H_d, H_k), 5.92 (H_a, H_b), 3.85−3.65 (H_g, H_i, H_h, H_j), 3.66−3.51 (H_j, H_h, H_g, H_i), 3.66−3.51 (H_u, H_x, H_v, H_w), 2.37 (H_q, H_t), 1.55 (H_x, H_w, H_u), 0.99 (H_t, H_q), 0.86 (H_v, H_u), −1.21 (H_w, H_x, H_u). Key ^{1}H−^{1}H NOESY: δ 7.95 (H_f, H_g, H_k), 7.62−7.59 (H_n, H_m, H_w, H_l, H_v), 7.57 (H_r, H_q), 7.51 (H_p, H_j, H_a), 7.20 (H_e, H_l), 6.82 (H_b, H_x, H_u), 6.59 (H_k, H_f, H_i, H_t), 6.52−6.48 (H_c, H_l, H_t, H_m, H_e), 5.92 (H_a, H_p, H_x, H_h), 3.85−3.65 (H_g, H_i, H_k, H_f), 3.66−3.51 (H_j, H_h, H_x, H_a, H_p), 3.66−3.51 (H_u, H_x, H_v, H_b, H_q), 2.37 (H_q, H_v, H_u, H_r), 1.55 (H_x, H_w, H_u), 0.99 (H_t, H_s, H_c, H_k), 0.86 (H_v, H_u, H_q, H_w, H_n, H_m), −1.21 (H_w, H_x, H_v, H_n, H_m).

Data for 6e. ^{1}H NMR (CD_2Cl_2): δ 7.85 (d, J = 8.7 Hz, 1 H, H_f), 7.56 (d, J = 8.1 Hz, 1 H, H_r), 7.49−7.42 (m, 2 H, H_p, H_n), 7.29−7.23 (m, 3 H, H_b, H_o, H_m), 7.18 (dd, J = 7.7, 6.6 Hz, 1 H, H_e), 7.09 (d, J = 8.1 Hz, 1 H, H_q), 7.05 (d, J = 8.7 Hz, 1 H, H_c), 6.73 (dd, 7.8, 6.5 Hz, 1 H, H_d), 6.70 (d, J = 3.1 Hz, 1 H, H_k), 6.21 (d, J = 3.1 Hz, 1 H, H_l), 6.00 (d, J = 3.1 Hz, 1 H), 3.99−3.91 (m, 2 H, H_g, H_i), 3.65−3.61 (m, 2 H, H_h, H_j), 3.61−3.46 (m, 1 H, H_u), 2.09 (s, 3 H, H_s), 1.09 (d, J = 5.0 Hz, 3 H, H_v), 1.00 (s, 3 H, H_t), 0.43 (dd, J = 12.9, 5.0, 1 H, H_x), −0.23 (dd, J = 12.9, 11.5 Hz, 1 H, H_w). ^{13}C{^{1}H} NMR (CD_2Cl_2): δ 167.8 (C2″), 157.7 (C6″), 143.4 (C4″), 133.1 (C5″), 130.5 (C4′), 128.5 (C5′), 127.5 (C9), 127.4 (C4′), 127.3 (C6), 126.4 (C8), 126.2 (C5), 126.1 (C8′), 125.8 (C6′), 124.3 (C7′), 123.7 (C4), 123.5 (C3″), 123.4 (C1′), 122.5 (C1), 121.4 (C7), 116.6 (C2), 115.2 (C2′), 108.7 (C3), 103.5 (C3′), 67.0 (C7″), 39.2 (C8″), 28.9 (C10′), 28.5 (C10), 24.8 (CH_3 on C6″), 22.9 (C9″), 17.9 (CH_3 on C5″). Key ^{1}H−^{1}H COSY correlations: δ 7.85 (H_f, H_e), 7.56 (H_r, H_q), 7.49−7.42 (H_p, H_n, H_o, H_m), 7.29−7.23 (H_o, H_m, H_p, H_n), 7.29−7.23 (H_b, H_a), 7.18 (H_e, H_d, H_f), 7.09 (H_q, H_r), 7.05 (H_c, H_d), 6.73 (H_d, H_c, H_e), 6.70 (H_k, H_l), 6.21 (H_l, H_k), 6.00 (H_a, H_b), 3.99−3.91 (H_g, H_i, H_h, H_j), 3.65−3.61 (H_h, H_j, H_g, H_i), 3.61−3.61 (H_u, H_x, H_w, H_v), 2.09 (H_s, H_t), 1.09 (H_v, H_u), 1.00 (H_v, H_s), 0.43 (H_x, H_u, H_w), −0.27 (H_w, H_x, H_u). Key ^{1}H−^{1}H NOESY correlations: δ 7.85 (H_f, H_g), 7.56 (H_r, H_s), 7.49−7.42 (H_p, H_n, H_j, H_w), 7.29−7.23 (H_o, H_m, H_w, H_p), 7.29−7.23 (H_b, H_x, H_u), 7.18 (H_e, H_d, H_f), 7.09 (H_q, H_v, H_u), 7.05 (H_c, H_b, H_t), 6.73 (H_d, H_t), 6.70 (H_k, H_i, H_t), 6.21 (H_l, H_m, H_t), 6.00 (H_a, H_h, H_p, H_x), 3.99−3.91 (H_g, H_i, H_f, H_k), 3.65−3.61 (H_h, H_j, H_a, H_p), 3.61−3.61 (H_u, H_x, H_v, H_b, H_q), 2.09 (H_s, H_r), 1.09 (H_v, H_w, H_b, H_q), 1.00 (H_t, H_l, H_k), 0.43 (H_x, H_u, H_a, H_b), −0.27 (H_w, H_v, H_n, H_m).

Data for 6e′. ^{1}H NMR (CD_2Cl_2): δ 6.95 (dd, 1 H), 6.59 (d, J = 3.1 Hz, 1 H, H_l), 6.30 (d, J = 3.1 Hz, 1 H, H_k), 2.76 (m, 1 H, H_u), 2.48 (dd, 1 H, H_x), 2.09 (s, 3 H, H_s), 1.18 (d, J = 6.8 Hz, 1 H, H_v), 0.77 (s, 3 H, H_t), −1.79 (dd, J = 13.3, 3.1, 1 H). ^{13}C{^{1}H} NMR (CD_2Cl_2): δ 168.1 (C2″), 118.04 (C3′), 103.8 (C2′), 67.9 (C7″), 43.0 (C8″), 23.7 (CH_3 on C6″), 23.4 (C9″). Key ^{1}H−^{1}H COSY correlations: δ 6.59 (H_l, H_k), 6.30 (H_k, H_l), 2.76 (H_u, H_x, H_v, H_w), 2.48 (H_x, H_u, H_w), 1.18 (H_v, H_q), 0.77 (H_t, H_q), −1.79 (H_w, H_x, H_u). Key ^{1}H−^{1}H NOESY correlations: δ 6.59 (H_l, H_t), 6.30 (H_k, H_t), 2.76 (H_u, H_q), 2.48 (H_x, H_w), 1.18 (H_v, H_q), 0.77 (H_t, H_k, H_l), −1.79 (H_w, H_u).

Data for 6f. ^{1}H NMR (CD_2Cl_2): δ 7.71 (d, J = 8.7 Hz, 1 H, H_f), 7.64 (d, J = 8.7 Hz, 1 H, H_m), 7.51−7.46 (dd, 1 H, H_n), 7.41 (s, 1 H, H_r), 7.30−7.15 (m, 3 H, H_b, H_o, H_p), 7.07 (dd, J = 7.6, 6.6 Hz, 1 H, H_e), 6.87 (d, J = 3.6 Hz, 1 H, H_k), 6.62 (d, J = 8.7 Hz, 1 H, H_c), 6.34 (dd, 1 H, H_d), 6.35 (d, J = 3.2 Hz, 1 H, H_l), 5.95 (d, J = 3.3 Hz, 1 H, H_a), 5.89 (s, 1 H, H_t), 4.10−4.00 (m, 2 H, H_g, H_i), 3.70−3.55 (m, 3 H, H_u, H_j, H_h), 2.28 (s, 3 H, H_q), 2.13 (s, 3 H, H_s), 1.85 (dd, J = 13.7, 9.0, 1 H, H_x), 0.95 (d, J = 7.2 Hz, 1 H, H_v), −1.48 (dd, J = 13.6, 5.0 Hz, 1 H, H_w). ^{13}C{^{1}H} NMR (CD_2Cl_2): δ 166.9 (C2″), 145.3 (C4″), 141.9 (C6″), 134.6 (C3″), 132.4 (C5″), 128.3 (C5), 127.8 (C8), 127.2 (C7′), 126.9 (C8′), 126.8 (C4′), 126.5 (C6), 126.3 (C5), 124.1 (C9), 123.1 (C7′), 122.9 (C4), 122.8 (C1), 122.4 (C9′), 122.2 (C1′), 120.4 (C7), 117.7 (C2), 116.8 (C2′), 109.3 (C3), 109.1 (C3′), 60.6 (C7″), 41.2 (C8″), 29.1 (C10), 28.4 (C10′), 24.5 (C9″), 19.0 (CH_3 pyridyl on C5″), 17.1 (CH_3 pyridyl on C3″). Key ^{1}H−^{1}H COSY correlations: δ 7.71 (H_f, H_e), 7.64 (H_m, H_n), 7.51−7.46 (H_n, H_o, H_m), 7.41 (H_r, H_t), 7.30−7.15 (H_o, H_p, H_n), 7.30−7.15 (H_b, H_a), 7.07 (H_e, H_d, H_f), 6.87 (H_k, H_l), 6.62 (H_c, H_d), 6.34 (H_d, H_e, H_c), 6.35 (H_l, H_k), 5.95 (H_a, H_b), 5.89 (H_t, H_r), 4.10−4.00 (H_g, H_i, H_h, H_j), 3.70−3.55 (H_j, H_h, H_g, H_i), 3.70−3.55 (H_u, H_x, H_w, H_v), 2.28 (H_q, H_r, H_t), 2.13 (H_s, H_r, H_t), 1.85 (H_x, H_w, H_u), 0.95 (H_v, H_u), −1.48 (H_w, H_x, H_u). Key ^{1}H−^{1}H NOESY correlations: δ 7.71 (H_f, H_k, H_j), 7.64 (H_m, H_l, H_v), 7.51−7.46 (H_n, H_o, H_m), 7.41 (H_r, H_s, H_q), 7.30−7.15 (H_o, H_p, H_n, H_h, H_j), 7.30−7.15 (H_b, H_u, H_x), 7.07 (H_e, H_d, H_f), 6.87 (H_k, H_t, H_f), 6.62 (H_c, H_b), 6.34 (H_d, H_t), 6.35 (H_l, H_t, H_m), 5.95 (H_a, H_h, H_x), 5.89 (H_t, H_k, H_l, H_d), 4.10−4.00 (H_g, H_i, H_f, H_k), 3.70−3.55 (H_j, H_h, H_a, H_p), 3.70−3.55 (H_u, H_x, H_v), 2.28 (H_q, H_u, H_v), 2.13 (H_s, H_r, H_t), 1.85 (H_x, H_u, H_b), 0.95 (H_v, H_q, H_m), −1.48 (H_w, H_x, H_v).

Data for 6f′. ^{1}H NMR (CD_2Cl_2): δ 7.83 (d, J = 8.7 Hz, H_f), 7.78 (d, J = 3.3 Hz, 1 H, H_b), 7.55−7.50 (m, 2 H, H_n, H_o), 7.40 (s, 1 H, H_r), 7.35 (d, J = 8.1 Hz, 1 H, H_m), 7.30−7.27 (m, 1 H), 7.19 (d, J = 7.7 Hz, 1 H, H_c), 6.95 (d, J = 3.5 Hz, 1 H, H_k), 6.80 (dd, J = 8.7, 6.7 Hz, 1 H, H_d), 5.98 (d, J = 3.4 Hz, 1 H, H_a), 5.73 (d, J = 3.2 Hz, 1 H, H_l), 5.54 (s, 1 H, H_t), 4.25−4.10 (m, 2 H, H_g, H_i), 3.90−3.60 (m, 2 H, H_h, H_j), 3.45−3.33 (m, 1H, H_u), 2.17 (s, 3 H, H_q), 2.11 (s, 3 H, H_s), 1.36 (d, J = 7.2 Hz, 3 H, H_v), 1.19 (dd, J = 13.7, 1.4 Hz, 1 H, H_x), −1.24 (dd, J = 13.7, 9.5 Hz, 1 H, H_w). ^{13}C{^{1}H} NMR (CD_2Cl_2): δ 166.68 (C2″), 144.5 (C4″), 142.4 (C6″), 134.3 (C3″), 133.6 (C5″), 128.3 (C6), 127.7 (C8), 127.5 (C7′), 127.3 (C6′), 127.2 (C5′), 126.7 (C8′), 125.9 (C5), 124.1 (C4), 123.4 (C9), 122.7 (C1), 122.6 (C9′, C4′), 121.6 (C1′), 120.4 (C7), 118.0 (C2), 116.1 (C2′), 110.4 (C3′), 108.8 (C3), 59.9 (C7″), 41.8 (C8″), 29.4 (C10), 27.7 (C10′), 24.2 (C9″), 18.2 (CH_3 pyridyl on C5″), 17.3 (CH_3 on C3″). Key ^{1}H−^{1}H COSY correlations: δ 7.83 (H_f, H_e), 7.78 (H_b, H_a), 7.55−7.50 (H_n, H_o, H_p, H_m), 7.40 (H_r, H_t), 7.35 (H_m, H_n), 7.30−7.27 (H_e, H_f, H_d), 7.19 (H_c, H_d), 6.95 (H_k, H_l), 6.80 (H_d, H_c, H_e), 5.98 (H_a, H_b), 5.54 (H_t, H_r), 3.45−3.33 (H_u, H_v, H_w), 2.17 (H_q, H_r, H_t), 2.11 (H_s, H_r, H_t), 1.36 (H_v, H_u), 1.19 (H_x, H_w), −1.24 (H_w, H_x, H_u). Key ^{1}H−^{1}H NOESY correlations: δ 7.83 (H_f, H_g, H_k), 7.78 (H_b, H_c, H_x, H_v), 7.55−7.50 (H_n, H_o, H_w, H_u), 7.40 (H_r, H_s, H_q), 7.35 (H_m, H_w), 7.30−7.27 (H_e, H_f, H_d), 7.19 (H_c, H_b, H_v), 6.95 (H_k, H_f, H_t, H_i), 6.80 (H_d, H_c, H_e), 5.98 (H_a, H_p, H_h, H_x), 5.54 (H_t, H_s, H_k), 3.45−3.33 (H_u, H_w, H_q), 2.17 (H_q, H_u, H_v), 2.11 (H_s, H_r, H_t), 1.36 (H_v, H_q, H_b, H_c), 1.19 (H_x, H_a, H_b), −1.24 (H_w, H_x, H_u).

Synthesis of [6a/6a′][BPh$_4$]. [*rac*-(EBI)Zr(η^2-6-methylpyrid-2-yl)(2-methylpyridine)][BPh_4] (0.170 g, 0.200 mmol) was added to CH_2Cl_2 (3 mL). The yellow solution that formed was exposed to propene (56.6 mL at 1 atm, 11.8 equiv, 23 °C) through a connected gas bulb with a Teflon valve. The volatiles were removed under vacuum, yielding a yellow oil. Hexane (10 mL) was added to give a yellow precipitate. The suspension was stirred for 4 h, and the solid was isolated by filtration, washed with hexane (3 × 2 mL), and dried under

vacuum. Yield: 0.15 g (94%). Anal. Calcd for $C_{53}H_{48}BNZr$: C, 79.47; H, 6.04; N, 1.75. Found: C, 79.36; H, 6.05; N, 1.67. The NMR data for [**6a**/**6a′**][BPh_4] are identical with the data for [**6a**/**6a′**][$MeB(C_6F_5)_3$], with the exception of the anion resonances.

Hydrolysis of 6d, 6e/6e′, and 6f/6f′. Solutions of **6d** and **6e**/**6e′** and **6f/6f′** in CD_2Cl_2 were generated by the reaction of propene with **5d**−**f** at 23 °C as described above. Water (0.7 μL, 0.04 mmol) was added, resulting in the immediate formation of a yellow precipitate. The suspension was filtered through glass wool, and the filtrate was analyzed by ^{1}H NMR and GC−MS, which showed the presence of free (EBI)H_2 and the single pyridine derivative **8d**−**f**.

Data for 8d. ^{1}H NMR (CD_2Cl_2): δ 7.70 (d, J = 7.5 Hz, 1 H, pyridine ring), 6.86 (d, J = 7.6 Hz, 1 H, pyridine ring), 3.18 (septet, J = 6.8 Hz, CH isopropyl), 2.73 (s, 3 H, CH_3 pyridine), 2.43 (s, 3 H, CH_3 pyridine), 1.13 (d, J = 6.9 Hz, 6 H, 2 CH_3 isopropyl). MS (*m*/*z*) 149 (M^+, 37), 148 (M-1$^+$, 41), 134 (M-15$^+$, 100).

Data for 8e. ^{1}H NMR (CD_2Cl_2): δ 7.81 (d, J = 7.4 Hz, 1 H, pyridine ring), 7.33 (d, J = 7.2 Hz, 1H, pyridine), 6.94 (d, J = 7.5 Hz, 1 H), 3.09 (septet, J = 6.6 Hz, CH isopropyl), 2.69 (s, 3 H, CH_3 pyridine), 2.37 (s, 3 H, CH_3 pyridine), 1.02 (d, J = 6.3 Hz, 6 H, 2 CH_3 isopropyl). MS (*m*/*z*): 149 (M^+, 31), 148 (M − 1$^+$, 48), 134 (M − 15$^+$, 100).

Data for 8f. ^{1}H NMR (CD_2Cl_2): δ 8.51 (s, 1 H, pyridine ring), 7.31 (s, 1 H, pyridine ring), 3.00 (septet, J = 6.1 Hz, CH isopropyl), 2.42 (s, 3 H, CH_3 pyridine), 2.31 (s, 3 H, CH_3 pyridine), 1.01 (d, J = 6.1 Hz, 6 H, 2 CH_3 isopropyl). MS (*m*/*z*): 149 (M^+, 28), 148 (M − 1$^+$, 42), 134 (M − 15$^+$, 100).

Propene Insertion of 5a and 5e at −88 °C. *rac*-(EBI)-$ZrMe_2$ (15.1 mg, 0.040 mmol), $B(C_6F_5)_3$ (20.5 mg, 0.040 mmol) and CD_2Cl_2 (0.5 mL) were added to a resealable NMR tube and vigorously mixed. In a drybox, the appropriate pyridine (0.040 mmol) was added, and the tube was shaken and then opened to release CH_4. Outside the drybox, the tube was attached to a vacuum line via a gas bulb. The solution was frozen at −196 °C (liquid N_2), the tube was evacuated, and propene (0.400 mmol, 10.0 equiv), measured *via* the gas bulb, was condensed into the tube. The tube was inserted in a −88 °C precooled NMR probe. After 1 h at −88 °C, the solution had thawed and a ^{1}H NMR spectrum was recorded. NMR data for **6a**/**6a′** and **6e**/**6e′** are listed above.

Propene Insertion of 5a−f at 80 °C. *rac*-(EBI)$ZrMe_2$ (15.1 mg, 0.040 mmol), $B(C_6F_5)_3$ (20.5 mg, 0.040 mmol), and C_6D_5Cl (0.5 mL) were added to a resealable NMR tube and vigorously mixed. In a drybox, the appropriate pyridine (0.040 mmol) was added, and the tube was shaken and then opened to release CH_4. *m*-Xylene (0.5 equiv) was added as an internal standard. The tube was attached to a vacuum line via a gas bulb. The tube was placed in a 80 °C preheated oil bath and exposed to propene (0.400 mmol, 10 equiv) via the gas bulb. The tube was maintained at 80 °C and periodically monitored by ^{1}H NMR. When the isomer ratio remained constant, the volatiles were removed under vacuum, CD_2Cl_2 was added by vacuum transfer, and ^{1}H and ^{13}C{^{1}H} NMR spectra were recorded. In the case of **5d**, 2D NMR experiments were also performed. For NMR characterization of **6d**, see above.

Data for 6d′. ^{1}H NMR (CD_2Cl_2): δ 3.30 (m, 1 H, H_u), 1.80 (s, 3 H, H_q), 1.31 (dd, J = 12.9 Hz, 1 H, H_x), 1.11 (d, 3 H, H_v), 0.41 (s, 3 H, H_t), −1.73 (dd, J = 12.9, 9.4 Hz, 1 H, H_w). ^{13}C-{^{1}H} NMR: δ 61.5 (C7″), 41.3 (C8″), 26.0 (CH_3 on C6″), 24.9 (C9″), 18.5 (CH_3 on C3″). Key ^{1}H−^{1}H COSY correlations: δ 3.30 (H_u, H_x, H_v, H_w), 1.31 (H_x, H_w, H_u), 1.11 (H_v, H_u), −1.73 (H_w, H_x, H_u). Key ^{1}H−^{1}H NOESY correlations: δ 3.30 (H_u, H_x, H_v), 1.80 (H_q, H_u, H_v), 1.31 (H_x, H_w, H_v), 1.11 (H_v, H_u, H_x), −1.73 (H_w, H_x).

Data for 6d″. ^{1}H NMR (CD_2Cl_2): δ 6.87 (d, J = 7.8 Hz, 1 H, H_s), 6.82 (d, J = 3.1 Hz, 1 H, H_b), 6.76 (dd, J = 7.6, 6.6 Hz, 1 H, H_d), 6.59 (d, J = 3.1 Hz, 1 H), 3.22 (dd, J = 12.3, 7.2 Hz, 1 H, H_w), 2.91 (dd, J = 12.3, 11.7 Hz, 1 H, H_x), 2.18 (s, 3 H, H_q), 1.40 (s, 3 H, H_t), 0.86 (d, J = 6.8 Hz, 3 H, H_v), 0.85 (m, 1 H, H_u). ^{13}C{^{1}H} NMR: δ 169.0 (C2″), 131.8 (ipso), 120.0 (C2), 107.8 (C3), 66.7 (C7″), 41.1 (C8″), 29.5, 27.5, 25.6 (C9″), 24.8, (CH_3 on C6″). Key ^{1}H−^{1}H COSY correlations: δ 3.22 (H_w, H_x, H_u), 2.91 (H_x, H_w, H_u), 2.18 (H_q, H_t), 1.40 (H_t, H_q), 0.86 (H_v, H_u), 0.85 (H_u, H_v, H_x, H_w). Key ^{1}H−^{1}H NOESY correlations: δ 3.22 (H_w, H_u, H_q), 2.91 (H_x, H_w, H_b), 2.18 (H_q, H_w, H_r), 0.86 (H_v, H_u, H_a, H_b), 0.85 (H_u, H_v, H_w).

Hydrolysis of 6d/6d′/6d″. H_2O was added to a C_6D_5Cl solution (0.5 mL, 0.04 mmol) of the thermodynamic **6d**/**6d′**/**6d″** mixture, and a yellow precipitate formed immediately. The suspension was filtered through glass wool, and the filtrate was analyzed by ^{1}H NMR and GC−MS, which showed the presence of (EBI)H_2 and the two pyridines **8d** and **8d″**. Data for **8d** are listed above.

Data for 8d″. ^{1}H NMR (CD_2Cl_2): δ 7.68 (d, J = 7.6 Hz, 1 H, pyridine), 7.42 (d, J = 7.7 Hz, 1H, pyridine), 2.90 (t, J = 7.9 Hz, 2H, CH_2 propyl), 2.79 (s, 3H, CH_3), 2.51 (s, 3H, CH_3), 0.78 (m, 5H, CH_2CH_3). MS (*m*/*z*, (relative intensity))149 (M^+, 49), 120 (M − 29$^+$, 100).

Generation of 9a,b,e from 6a/6a′, 6b, and 6e/6e′. A C_6D_5-Cl solution (0.5 mL) of **6a**/**6a′**, **6b**, or **6e**/**6e′** (0.040 mmol) was added to a resealable NMR tube. The tube was cooled to −196 °C (liquid N_2), and 2-butyne (0.080 mmol, 2 equiv), measured by a gas bulb, was condensed in. The mixture was maintained at 23 °C and periodically monitored by ^{1}H NMR. After 15 h, the NMR tube was placed in a temperature bath regulated at 80 °C. The sample was periodically monitored by ^{1}H NMR (at ambient probe temperature). After 3 h, the reaction was complete and the final product was identified by ^{1}H and {^{1}H}^{13}C NMR.

Data for 9a. ^{1}H NMR (CD_2Cl_2): δ 7.79 (d, J = 8.64 Hz, 1 H), 7.74 (t, J = 7.9 Hz, 1 H), 7.67 (d, J = 8.6 Hz, 1 H), 7.46 (d, J = 8.6 Hz, 1 H), 7.33 (dd, J = 7.6, 6.7 Hz, 1 H), 7.20−7.12 (m, 3 H), 6.96 (d, J = 8.6 Hz, 1 H), 6.87 (d, J = 7.6 Hz, 1 H), 6.65 (dd, J = 7.5, 5.5 Hz, 1 H), 6.55 (d, J = 3.2 Hz, 1 H, indenyl C_5), 6.48 (d, J = 3.2 Hz, 1 H, indenyl C_5), 6.28 (d, J = 3.4 Hz, 1 H, indenyl C_5), 4.04−3.69 (m, 4 H, CH_2CH_2), 1.73 (s, 3 H), 1.59 (s, 3H), 1.39 (s, 3 H). ^{13}C{^{1}H} NMR (CD_2Cl_2): δ 214.2, 171.1, 142.7, 129.2, 128.7, 127.2, 126.4, 126.0, 124.1, 123.2, 122.9, 121.8, 118.2, 118.05, 116.1, 110.4, 105.7, 29.8, 28.4, 25.8, 22.8, 14.6.

Data for 9b. ^{1}H NMR (CD_2Cl_2): δ 8.03 (d, J = 8.7 Hz, 1 H), 7.92 (t, J = 7.9 Hz, 1 H), 7.01 (d, 3.1 Hz, 1 H), 6.98 (dd, J = 7.6, 6.6 Hz, 1 H), 6.78−6.34 (m, 10H), 6.12 (d, J = 3.1 Hz, 1 H), 6.01 (m, 2 H), 5.34 (d, J = 3.3 Hz, 1 H), 4.73 (d, J = 3.2 Hz, 1 H), 3.82−3.48 (m, 4 H, CH_2CH_2), 1.80 (s, 3 H), 1.43 (s, 3 H). ^{13}C{^{1}H} NMR (CD_2Cl_2): δ 217.9, 176.5, 142.8, 133.0, 132.3, 129.3, 128.5, 127.8, 127.5, 127.4, 126.8, 125.5, 125.2, 124.2, 124.1, 123.9, 123.0, 121.9, 119.5, 116.8, 115.9, 110.4, 106.7, 29.3, 29.0, 25.3, 15.0.

Data for 9e. ^{1}H NMR (CD_2Cl_2): δ 7.83 (d, J = 8.7 Hz, 1 H), 7.67 (d, J = 8.6 Hz, 1 H), 7.60 (d, J = 8.3 Hz, 1 H), 7.38 (d, J = 8.6 Hz, 1 H), 7.30 (dd, J = 6.7, 6.5 Hz, 1 H), 7.18 (dd, J = 6.4, 6.2 Hz, 1 H), 7.19−7.10 (m, 32 H), 6.97 (d, J = 8.5 Hz, 1 H), 6.68 (dd, J = 6.6, 6.1 Hz, 1 H), 6.61 (d, J = 3.2 Hz, 1 H, indenyl C_5), 6.35 (d, J = 3.1 Hz, 1 H, indenyl C_5), 6.24 (d, J = 3.4 Hz, 1 H, indenyl C_5), 4.00−3.67 (m, 4 H, CH_2CH_2), 2.12 (s, 3 H), 1.72 (s, 3 H), 1.32 (s, 3 H), 1.11 (s, 3 H). ^{13}C{^{1}H} NMR (CD_2Cl_2): δ 213.4, 170.9, 159.6, 155.5, 145.6, 145.5, 134.1, 133.1, 131.0, 130.4, 129.9, 129.5, 129.1, 128.2, 127.8, 127.7, 127.6, 125.9, 125.8, 125.5, 123.7, 123.6, 120.6, 119.4, 118.0, 111.8, 107.7, 31.3, 30.5, 26.8, 24.0, 19.9, 16.5.

Generation of 9a,b,e from *rac*-(EBI)$ZrMe_2$. *rac*-(EBI)-$ZrMe_2$ (15.1 mg, 0.040 mmol), $B(C_6F_5)_3$ (20.5 mg, 0.0400 mmol), and CH_2Cl_2 were added to a resealable NMR tube and vigorously mixed. In a dry box, the appropriate pyridine (0.040 mmol) was added and the NMR tube was shaken and then opened to release CH_4. On a vacuum line, the tube was cooled to −196 °C (liquid N_2) and 2-butyne (0.080 mmol, 2 equiv), measured by gas bulb, was condensed in. The tube was maintained at 23 °C for 1 h. The volatiles were removed under

high vacuum, CD_2Cl_2 was vacuum-transferred in, and ^1H and $^{13}C\{^1H\}$ NMR spectra were recorded.

Hydrolysis of 9a. Water (0.7 μL, 0.040 mmol) was added to a CD_2Cl_2 solution (0.5 mL) of **9a** (0.040 mmol). A yellow precipitate formed immediately. The suspension was filtered through glass wool, and the filtrate was analyzed by ^1H NMR and GC−MS, which showed the presence of $(EBI)H_2$ and the single pyridine **11a**.

Data for 11a. ^1H NMR (CD_2Cl_2): δ 6.81 (dd, ^3J = 7.8, 6.9 Hz, 1H), 6.53 (d, ^3J = 7.7 Hz, 1H), 6.41 (d, ^3J = 6.6 Hz, 1H), 6.07 (dd, J = 6.4, 2.1 Hz, 1 H), 2.51 (s, 3 H), 2.41 (d, J = 6.5 Hz, 3 H), 2.30 (s, 3 H). MS (m/z): 147 (M^+).

Molecular Modeling Calculations. All calculations were performed on a Silicon Graphics Indigo workstation with a R4000 processor running the IRIX operating system, using the software package Cerius[2] (version 2.1, Molecular Simulations, Inc.) The universal force field (UFF) developed by Rappé was used in all dynamics and mechanics runs.[18] The parameters used to generate the UFF include a set of hybridization-dependent atomic bond radii, a set of hybridization angles, van der Waals parameters, torsional and inversion barriers, and a set of effective nuclear charges.

A cationic zirconium complex was built with the molecule sketcher module in Cerius[2]. The overall charge of the complex was set with the "Open Force Field Setup-Charges-Average To" option. The EBI ligand was constructed by fusing cyclopentadienyl ligands with phenyl rings and bridging them with an ethylene unit. The hybridization of the Zr atom was defined as "Other". The Zr−C and Zr−N bond involving the η^2-pyridyl ligands in **12** and **12′** were defined as "Single", and distances were constrained to distances taken from $Cp_2Zr(\eta^2(C,N)$-6-methylpyrid-2-yl)$(PMe_3)^+$ crystallographic data.[2b] The Zr−N bonds involving the pyridine−alkyl ligands in **6** and **6′** were defined as "Single", and the distances were constrained to distances taken from *rac*-(EBI)Zr{η^2(*C*,*N*)-CH_2CH(Bu)(6-methylpyridyl)}$^+$ crystallographic data.[3,11] The centroid−Zr−centroid angle was also constrained to the angle in *rac*-(EBI)Zr{η^2(*C*,*N*)-CH_2CH(Bu)(6-methylpyridyl)}$^+$. All restraints were implemented by the "Open Force Field Setup-Energy Terms-Restraints" package. These restraints had a 1000 kcal mol^{-1} Å^{-2} force constant and obeyed a harmonic potential function. For the olefin adducts, the Zr−olefin bond was not defined, but rather the Zr−C distances were constrained to distances taken from *rac*-(EBI)Zr($OCMe_2CH_2CH_2CH{=}CH_2)^+$ crystallographic data.[20] For all complexes, only the *S*,*S* enantiomer was constructed.

As the structure was constructed, it was minimized by conjugate gradient methods to a 0.1 kcal mol^{-1} Å^{-1} root-mean-square force after the construction of each major ligand (EBI, pyridine, and propene). After complete construction, it was subjected to 5 ps of canonical ensemble (NVT: constant mole number, volume, and temperature) dynamics at 500 K to sample more configurational space and find a global energy minimum. Finally, this structure was again minimized using the same conditions as above.

Configurations of the molecule were taken every 5 ps for 50 ps of NVT dynamics at 500 K. This was accomplished by saving the structure after 10 continuous 5 ps runs. Each saved structure was then minimized by conjugate gradient methods to a 0.1 kcal mol^{-1} Å^{-1} root-mean-square force. The energy and several structural parameters of each minimized structure were analyzed by the "Measurements-Geometry" tool.

Acknowledgment. This work was supported by NSF Grant No. CHE-9413022. We are grateful to John Snyder for assistance with 2D NMR experiments, Nathan Baker for assistance with the molecular modeling, and Boulder Scientific for a gift of $B(C_6F_5)_3$.

OM970750Q